DTIC copy

AFRL-SN-HS-TR-2005-007

A LOW ORDER-SINGULARITY ELECTRIC-FIELD INTEGRAL EQUATION SOLVABLE WITH PULSE BASIS FUNCTIONS AND POINT MATCHING

Robert A. Shore
Arthur D. Yaghjian

In-House Technical Report: January 2001 – June 2004

APPROVED FOR PUBLIC RELEASE

AIR FORCE RESEARCH LABORATORY
Sensors Directorate
Electromagnetics Technology Division
80 Scott Drive
Hanscom AFB MA 01731-2909

TECHNICAL REPORT

A LOW ORDER-SINGULARITY ELECTRIC-FIELD INTEGRAL EQUATION SOLVABLE WITH PULSE BASIS FUNCTIONS AND POINT MATCHING

Unlimited, Statement A

NOTICE

USING GOVERNMENT DRAWINGS, SPECIFICATIONS, OR OTHER DATA INCLUDED IN THIS DOCUMENT FOR ANY PURPOSE OTHER THAN GOVERNMENT PROCUREMENT DOES NOT IN ANY WAY OBLIGATE THE US GOVERNMENT. THE FACT THAT THE GOVERNMENT FORMULATED OR SUPPLIED THE DRAWINGS, SPECIFICATIONS, OR OTHER DATA DOES NOT LICENSE THE HOLDER OR ANY OTHER PERSON OR CORPORATION; OR CONVEY ANY RIGHTS OR PERMISSION TO MANUFACTURE, USE, OR SELL ANY PATENTED INVENTION THAT MAY RELATE TO THEM.

THIS TECHNICAL REPORT HAS BEEN REVIEWED AND IS APPROVED FOR PUBLICATION.

//Signature//

Robert Shore
Project Manager, Antenna Technology Branch

//Signature//

Livio Poles
Chief, Antenna Technology Branch

//Signature//

Michael N. Alexander
Technical Adivsor
Electromagnetics Technology Division

REPORT DOCUMENTATION PAGE

Form Approved OMB No. 0704-0188

1. REPORT DATE *(DD-MM-YYYY)*		3. DATES COVERED *(From - To)*
25-06-2004	IN-HOUSE	1 January 2001 – 15 June 2004

4. TITLE AND SUBTITLE
A LOW-ORDER-SINGULARITY ELECTRIC-FIELD INTEGRAL EQUATION SOLVABLE WITH PULSE BASIS FUNCTIONS AND POINT MATCHING

5a. CONTRACT NUMBER

5b. GRANT NUMBER

5c. PROGRAM ELEMENT NUMBER

6. AUTHOR(S)
Robert A. Shore and Arthur D. Yaghjian

5d. PROJECT NUMBER
2304

5e. TASK NUMBER
HE

5f. WORK UNIT NUMBER
01

7. PERFORMING ORGANIZATION NAME(S) AND ADDRESS(ES)
AFRL/SNHA
80 Scott Drive
Hanscom AFB, MA 01731-2909

8. PERFORMING ORGANIZATION REPORT

9. SPONSORING / MONITORING AGENCY NAME(S) AND ADDRESS(ES)
Electromagnetics Technology Division
Sensors Directorate
Air Force Research Laboratory
80 Scott Drive
Hanscom AFB MA 01731-2909

10. SPONSOR/MONITOR'S ACRONYM(S)
AFRL/SNH A

11. SPONSOR/MONITOR'S REPORT NUMBER(S)

12. DISTRIBUTION / AVAILABILITY STATEMENT
Approved for public release; distribution unlimited. 1 October 2004, ESC 04-1003

13. SUPPLEMENTARY NOTES

14. ABSTRACT

Unlike the magnetic-field integral equation, the conventional form of the electric-field integral equation (EFIE) cannot be solved accurately with the method of moments (MOM) using pulse basis functions and point matching. The highly singular kernel of the EFIE , rather than the current derivatives, precludes the use of the pulse-basis function point-matching MOM. A new form of the EFIE has been derived whose kernel has no greater singularity than that of the free-space Green's function. This new low-order singularity form of the EFIE, the LEFIE, has been solved numerically for perfectly electrically conducting bodies of revolution (BORs) using pulse basis functions and point-matching. Derivatives of the current are approximated with finite differences using a quadratic Lagrangian interpolation polynomial. This simple solution of the LEFIE is contingent, however, on the vanishing of a linear integral that appears when the original EFIE is transformed to obtain the LEFIE. This generally restricts the applicability of the LEFIE to smooth closed scatterers. Bistatic scattering calculations performed for a prolate spheroid demonstrate that results comparable in accuracy to the conventional EFIE can be obtained with the LEFIE using pulse basis functions and point matching provided a higher density of points is used close to the ends of the BOR generating curve to compensate for the use of one-sided finite difference approximations of the first and second derivatives of the current.

15. SUBJECT TERMS
Electromagnetic scattering, electric-field integral equation, low-order singularity, body of revolution, perfect conductor

16. SECURITY CLASSIFICATION OF:			17.LIMITATION OF ABSTRACT	18.NUMBER OF PAGES	19a. NAME OF RESPONSIBLE PERSON Robert A. Shore
a. REPORT	b. ABSTRACT	c.THIS PAGE			19b. TELEPHONE NUMBER *(include area code)*
Unclassified	Unclassified	Unclassified	SAR	31	*781-377-2058*

Contents

1 INTRODUCTION 1

2 ANALYSIS 2

2.1 Derivation of the Low-Order Singularity Electric-Field Integral Equation 2

2.2 LEFIE for a BOR 5

2.3 Solution of the LEFIE by the Method of Moments 8

2.4 Expressions for the Elements of the Z Matrices 9

2.5 Expressions for the Elements of the V Vectors 17

2.6 Calculation of the Current 19

2.7 Calculation of the Far Scattered Field 20

2.8 Choice of the Number of Fourier Modes for Expansion and Testing Functions. 22

2.9 Approximation of Derivatives 23

3 NUMERICAL RESULTS 24

4 SUMMARY 27

REFERENCES 31

List of Figures

Figure 1. Body of revolution and coordinate system. 6
Figure 2. Plane wave scattering by a body of revolution. 7
Figure 3. Defining geometry for the angle v in the ρz plane. 11
Figure 4. Geometry of the prolate spheroid. 25
Figure 5. E-plane pattern of a prolate spheroid with $ka = 20$ and $kb = 10$ illuminated by a TM plane wave incident at an angle of 45° with the major axis, as calculated by the CFIE with a density of 40 points/λ, by the EFIE solved with overlapping triangle basis functions at a density of 20 points/λ, and by the EFIE solved with pulse basis functions and point matching at a density of 20 points/λ and 80 points/λ. 26
Figure 6. E-plane pattern of a prolate spheroid with $ka = 20$ and $kb = 10$ illuminated by a TM plane wave incident at an angle of 45° with the major axis, as calculated by the EFIE solved with overlapping triangle basis functions at a density of 20 points/λ, and by the LEFIE solved with pulse basis functions and point matching at a density of 40 points/λ and 20 points/λ. 28
Figure 7. E-plane pattern of a prolate spheroid with $ka = 20$ and $kb = 10$ illuminated by a TM plane wave incident at an angle of 45° with the major axis, as calculated by the EFIE solved with overlapping triangle basis functions at a density of 20 points/λ, by the LEFIE solved with pulse basis functions and point matching at a density of 80 points/λ in an interval of $\lambda/4$ at either end of the spheroid generating curve and 20 points/λ elsewhere, and by the LEFIE at a uniform density of 20 points/λ. 29

ACKNOWLEDGEMENT

This work was supported by the U.S. Air Force Office of Scientific Research (AFOSR).

1 INTRODUCTION

There are numerous commercial codes available that numerically solve electric-field integral equations (EFIE) for the current and scattered fields produced by an electromagnetic wave incident on a perfectly conducting (PEC) scatterer. For research purposes and for certain specialized geometries, however, it is often advantageous to have the flexibility and control inherent in writing one's own computer code. By far, the simplest approach for numerically solving integral equations is to use the method of moments (MOM) with pulse basis functions and point matching. Unfortunately, the EFIE, unlike the magnetic-field integral equation (MFIE), cannot be solved accurately using pulse basis functions and point matching (as demonstrated in Figure 5 below), and thus considerably more effort is required to write a computer code for numerically solving the EFIE. (It can be shown that it is the higher-order singularity of the EFIE kernel that prevents an accurate solution using pulse basis functions and point matching.) For open scatterers or many thin bodies the solution to the MFIE is inderminant or unstable, respectively, and it becomes necessary to use the EFIE. Moreover, because confidence in numerical solutions is greatly enhanced by having two independent numerical solutions that agree to within a certain accuracy, it is often highly desirable to obtain the solution to the EFIE even if the MFIE is also applicable.

The main purpose of this report is to derive a low-order singularity electric-field integral equation (LEFIE) that can be accurately solved using the MOM with pulse basis functions and point matching. This LEFIE, whose kernel, like that of the MFIE, has no singularity greater than that of the free-space Green's function, is solved numerically for perfectly conducting bodies of revolution (BORs) using pulse basis fucntions and point matching. Derivatives of the current are approximated with finite differences using a quadratic Lagrangian interpolation polynomial. This simple solution of the LEFIE is contingent, however, upon the vanishing of a line integral that appears when the original EFIE is transformed to obtain the LEFIE. This requirement generally restricts the simple applicability of the LEFIE to smooth closed surfaces. Bistatic scattering calculations performed for scattering of a plane wave by a prolate spheroid demonstrate that numerical results comparable in accuracy to the conventional EFIE can be obtained with the LEFIE using pulse basis functions and point matching, provided a higher density of points is used close to the ends of the BOR generating curve to compensate for the use of one-sided finite difference approximations of the first and second derivatives of the current.

The organization of the report is as follows. Section 2 contains the analysis of the low-order singularity electric-field integral equation (LEFIE) solution of the body of revolution (BOR) scattering problem. It is divided into several subsections beginning with the derivation of the general LEFIE in Section 2.1 and its restatement for a BOR in Section 2.2. The solution of the LEFIE for a closed BOR using pulse basis functions and point matching is outlined in Section 2.3. Detailed expressions for the elements of the Z matrices that multiply the column vectors of the surface current expansion function coefficients to be determined are derived in Section 2.4. The Z matrices are treated by expressing them as the sum of four submatrices corresponding to each of the four terms under the integral sign in the LEFIE. In Section 2.5 we obtain detailed expressions for the elements of the V column vectors in the right-hand side of the matrix equation formulation of the LEFIE. In Section 2.6 we obtain expressions for the currents induced on the surface of a BOR by a transverse electric

(TE) and transverse magnetic (TM) linearly polarized plane wave in terms of the solution to the LEFIE matrix equation, and in Section 2.7 expressions for the components of the far scattered field are derived. Section 2.8 discusses the choice of the number of Fourier modes that need to be used in the calculations. Section 2.9 treats the approximation of the current derivatives that appear in the formulation of the LEFIE.

Section 3 contains numerical results of calculations performed with a computer program written to implement and validate the solution of the LEFIE given in Section 2. A report summary is given in Section 4.

2 ANALYSIS

2.1 Derivation of the Low-Order Singularity Electric-Field Integral Equation

To derive the low-order singularity electric-field integral equation (LEFIE) we first derive the ordinary electric-field integral equation (EFIE) [1]. On the surface S of a PEC scatterer the total tangential electric field vanishes. The total field is expressed as the sum of the incident field and the scattered field, so that

$$\hat{\mathbf{n}}(\mathbf{r}) \times \mathbf{E}^{tot}(\mathbf{r}) = \hat{\mathbf{n}}(\mathbf{r}) \times [\mathbf{E}^{inc}(\mathbf{r}) + \mathbf{E}^{sc}(\mathbf{r})] = 0, \ \ \mathbf{r} \text{ on } S \tag{1}$$

where $\mathbf{E}^{tot}(\mathbf{r})$ and $\mathbf{E}^{sc}(\mathbf{r})$ are the total and scattered electric fields, respectively, $\hat{\mathbf{n}}$ is the unit normal vector to the surface S at the position $\mathbf{r}$, and $\hat{\mathbf{n}}$ is assumed directed outward from S. The scattered field can be expressed in terms of a vector potential $\mathbf{A}(\mathbf{r})$ and a scalar potential $\Phi(\mathbf{r})$ by

$$\mathbf{E}^{sc}(\mathbf{r}) = -j\omega\mathbf{A}(\mathbf{r}) - \nabla\Phi(\mathbf{r}) \tag{2}$$

where

$$\mathbf{A}(\mathbf{r}) = \mu_0 \int_S \mathbf{K}(\mathbf{r}')G(\mathbf{r},\mathbf{r}')dS' \tag{3}$$

and

$$\Phi(\mathbf{r}) = \frac{1}{\epsilon_0}\int_S \sigma(\mathbf{r}')G(\mathbf{r},\mathbf{r}')dS'. \tag{4}$$

Here $G(\mathbf{r},\mathbf{r}')$ is the free-space Green's function for harmonic time dependence $\exp(j\omega t)$ with the frequency $\omega > 0$. That is

$$G(\mathbf{r},\mathbf{r}') = G(\mid \mathbf{r}-\mathbf{r}' \mid) = \frac{\exp(-jk \mid \mathbf{r}-\mathbf{r}' \mid)}{4\pi \mid \mathbf{r}-\mathbf{r}' \mid} \tag{5}$$

where $\mathbf{r}$ and $\mathbf{r}'$ are the vectors to the field and source points respectively, $\mathbf{K}(\mathbf{r}')$ is the electric current on S to be determined, μ_0 and ϵ_0 are the permeability and permittivity of free space respectively, $k = \omega/c$ with c the speed of light in free space, and σ is the surface charge density given by

$$\sigma(\mathbf{r}') = -\frac{1}{j\omega}\nabla'_S \cdot \mathbf{K}(\mathbf{r}')\,. \tag{6}$$

The operator $\nabla'_S\cdot$ is the surface divergence [2, Appendix 2, 18.]. Combining (1) and (2), substituting (3), (4) and (6), letting the observation point $\mathbf{r}$ approach the surface S, and dividing by the free-space impedance $Z_0 = (\mu_0/\epsilon_0)^{1/2}$ we obtain

$$\frac{j}{k}\hat{\mathbf{n}}(\mathbf{r}) \times \oint_S [k^2\mathbf{K}(\mathbf{r}')G(\mathbf{r},\mathbf{r}') - (\nabla'_S \cdot \mathbf{K}(\mathbf{r}'))\nabla' G(\mathbf{r},\mathbf{r}')]dS' = \frac{\hat{\mathbf{n}}(\mathbf{r})}{Z_0} \times \mathbf{E}^{inc}(\mathbf{r}). \tag{7}$$

The "o" on the integral sign in (7) indicates that a small "principal area" isolates the singularity of the Green's function from the surface integration. The form of the EFIE in (7) is conditional upon the choice of the principal area being a circle with the singular point at its center (or another principal area that is adequately symmetric with respect to the singular point) [3]. Equation (7) is the conventional form of the EFIE for the current $\mathbf{K}$ on the surface S of a PEC scatterer.

The gradient operator acting on the free-space Green's function in (7) results in a higher order singularity, $1/|\mathbf{r}-\mathbf{r}'|^2$, instead of the $1/|\mathbf{r}-\mathbf{r}'|$ singularity for the free-space Green's function itself. What we want to do is to recast the conventional form of the EFIE into a new form that has no singularity higher than that of the free-space Green's function. To do this we begin by writing the gradient operating on the free-space Green's function as the sum of the surface gradient ∇'_S and the gradient in the normal direction so that (7) becomes

$$\frac{j}{k}\hat{\mathbf{n}}(\mathbf{r}) \times \oint_S [k^2\mathbf{K}(\mathbf{r}')G(\mathbf{r},\mathbf{r}') - (\nabla'_S \cdot \mathbf{K}(\mathbf{r}'))\nabla'_S G(\mathbf{r},\mathbf{r}') -$$

$$(\nabla'_S \cdot \mathbf{K}(\mathbf{r}'))\frac{\partial G(\mathbf{r},\mathbf{r}')}{\partial n'}\hat{\mathbf{n}}(\mathbf{r}')]dS' = \frac{\hat{\mathbf{n}}(\mathbf{r})}{Z_0} \times \mathbf{E}^{inc}(\mathbf{r}). \tag{8}$$

The term in (8) with the normal derivative of G includes the cross product $\hat{\mathbf{n}}(\mathbf{r}) \times \hat{\mathbf{n}}(\mathbf{r}')$ and does not have a singularity higher than G itself at $\mathbf{r} = \mathbf{r}'$. Focusing on the surface gradient term, we use the vector identity [2, Appendix 2, 26.]

$$\nabla_S(AB) = A\nabla_S B + B\nabla_S A \tag{9}$$

to write

$$(\nabla'_S \cdot \mathbf{K})\nabla'_S G = \nabla'_S[(\nabla'_S \cdot \mathbf{K})G] - G\nabla'_S(\nabla'_S \cdot \mathbf{K}). \tag{10}$$

We then use a Gauss integral theorem [2, Appendix 2, 43.] to obtain

$$\oint_S \nabla'_S[(\nabla'_S \cdot \mathbf{K})G]dS' = -\oint_S J'(\nabla'_S \cdot \mathbf{K})G\hat{\mathbf{n}}'dS' + \int_C (\nabla'_S \cdot \mathbf{K})G\hat{\mathbf{m}}'|dc'|. \tag{11}$$

In (11)

$$J' = \frac{1}{R'_1} + \frac{1}{R'_2} \tag{12}$$

where R'_1 and R'_2 are the principal radii of curvature at the surface point $\mathbf{r}'$, and C is a set of closed curves (defined below) on the surface of the PEC scatterer. The unit vector $\hat{\mathbf{m}}'$, defined at each point on the curves comprising C, is in the tangent plane to the surface at the point and perpendicular to the curve. Primes are used to denote dependence on the source point $\mathbf{r}'$.

Since (11) is the key step in obtaining a new form of the EFIE it is important to understand the meaning of S and C in applying it. We assume that the surface S of a general PEC scatterer can be divided into a finite number of open subsurfaces sharing bounding curves in common with one another, such that on each subsurface the surface charge density $\sigma(\mathbf{r}') = -1/(j\omega)\nabla'_S \cdot \mathbf{K}(\mathbf{r}')$, its surface derivative, and J' are continuous and integrable, and $\hat{\mathbf{n}}'$ and $\hat{\mathbf{m}}'$ are continuous. In applying (11) to the surface S of the PEC scatterer, S is to be regarded as the superposition of these subsurfaces, and the surface and line integrations performed separately for each subsurface with its bounding curve. The set of bounding curves comprise C. The unit vector $\hat{\mathbf{m}}'$ on each of the bounding curves comprising C points away from the subsurface it encloses. The surface of a closed finite cylinder, for example, is to be regarded as the superposition of three subsurfaces, the side cylindrical surface and the two disks at either end. The surface of a sphere, a simple smooth scatterer, can be regarded as the superposition of two hemispheres.

Combining (8) and (11) we obtain a new form of the EFIE with a self-term singularity equal to that of the free-space Green's function

$$\frac{j}{k}\hat{\mathbf{n}}(\mathbf{r}) \times \oint_S \{[k^2\mathbf{K}(\mathbf{r}') + \nabla'_S(\nabla'_S \cdot \mathbf{K}(\mathbf{r}')) + J'(\nabla'_S \cdot \mathbf{K}(\mathbf{r}'))\hat{\mathbf{n}}(\mathbf{r}')]G(\mathbf{r},\mathbf{r}')$$

$$-(\nabla'_S \cdot \mathbf{K}(\mathbf{r}'))\frac{\partial G(\mathbf{r},\mathbf{r}')}{\partial n'}\hat{\mathbf{n}}(\mathbf{r}')\}dS' - \frac{j}{k}\hat{\mathbf{n}}(\mathbf{r}) \times \int_C (\nabla'_S \cdot \mathbf{K}(\mathbf{r}'))G(\mathbf{r},\mathbf{r}')\hat{\mathbf{m}}(\mathbf{r}')|dc'|$$

$$= \frac{\hat{\mathbf{n}}(\mathbf{r}) \times \mathbf{E}^{inc}(\mathbf{r})}{Z_0} \tag{13}$$

which, unlike the original EFIE in (7), is not conditional upon the shape of the principal area used to isolate the singularity of the Green's function.

Now our recasting of the conventional EFIE (7) into this new low-order singularity form (13) is motivated by the desire to be able to solve the EFIE with the method of moments using pulse basis functions and point matching. Therefore we would like to avoid the line integral over C in (13). Assume that the surface S of the scatterer is closed and smooth enough so that $\sigma(\mathbf{r}') = -1/(j\omega)\nabla'_S \cdot \mathbf{K}(\mathbf{r}')$, its surface derivative, and J' are continuous and bounded, and $\hat{\mathbf{n}}'$ and $\hat{\mathbf{m}}'$ are continuous over S. Then (13) can be applied to any two contiguous open surfaces (with a smooth bounding curve) comprising the closed surface, the two line integrals over the common bounding curve of the two contiguous surfaces cancel, and (13) reduces to

$$\frac{j}{k}\hat{\mathbf{n}}(\mathbf{r}) \times \oint_S \{[k^2\mathbf{K}(\mathbf{r}') + \nabla'_S(\nabla'_S \cdot \mathbf{K}(\mathbf{r}')) + J'(\nabla'_S \cdot \mathbf{K}(\mathbf{r}'))\hat{\mathbf{n}}(\mathbf{r}')]G(\mathbf{r},\mathbf{r}')$$

$$-(\nabla'_S \cdot \mathbf{K}(\mathbf{r}'))\frac{\partial G(\mathbf{r},\mathbf{r}')}{\partial n'}\hat{\mathbf{n}}(\mathbf{r}')\}dS' = \frac{\hat{\mathbf{n}}(\mathbf{r}) \times \mathbf{E}^{inc}(\mathbf{r})}{Z_0}. \tag{14}$$

If the scatterer has an open surface, edges, tips, or any boundary where σ or J' become singular or discontinuous, or $\hat{\mathbf{n}}'$ and $\hat{\mathbf{m}}'$ become discontinuous, the line integral over C cannot, in general, be omitted and the numerical solution to the low-order singularity electric-field integral equation (LEFIE) (13) may be more complicated than that of the original EFIE.

Accordingly we will restrict our treatment of the LEFIE in this report to PEC scatterers with closed smooth surfaces such as spheroids for which σ, its surface derivative, and J' are continuous and bounded, and $\hat{\mathbf{n}}'$ and $\hat{\mathbf{m}}'$ are continuous, so that the line integral over C can be omitted and the LEFIE takes the form (14).

2.2 LEFIE for a BOR

We seek to determine the surface current and the far scattered field of a perfectly electrically conducting (PEC) closed body of revolution (BOR) excited by an incident plane wave. The geometry of the BOR is shown in Figure 1. Circular cylinder coordinates (ρ, ϕ, z) are employed with $(\hat{\boldsymbol{\rho}}, \hat{\boldsymbol{\phi}}, \hat{\mathbf{z}})$ denoting the corresponding unit vectors, and with the z axis chosen as the axis of revolution. The origin of the circular cylindrical coordinate system lies on the z axis but does not necessarily coincide with the lower pole of the BOR as in Figure 1. The coordinates (t, ϕ), with t the path length along the generating curve of the BOR from the lower pole, form an orthogonal curvilinear system on the surface S of the BOR; the corresponding unit vectors are $(\hat{\mathbf{t}}, \hat{\boldsymbol{\phi}})$. Figure 2 shows the propagation vector $\mathbf{k}^{inc} = k\,\hat{\mathbf{k}}^{inc}$ of the incident plane wave. The propagation vector is assumed to lie in the xz plane ($\phi = 0$), with $-\hat{\mathbf{k}}^{inc}$ making an angle of θ^{inc} with the positive z axis and with $k_x{}^{inc} \leq 0$ so that

$$\mathbf{k}^{inc} = -k(\sin\theta^{inc}\hat{\mathbf{x}} + \cos\theta^{inc}\hat{\mathbf{z}}). \tag{15}$$

Also shown in Figure 2 are the spherical polar angles of the far field observation point $\mathbf{r}^{far} = (r, \theta^{far}, \phi^{far})$ and the associated unit vectors $\hat{\boldsymbol{\theta}}^{far}$ and $\hat{\boldsymbol{\phi}}^{far}$. For TM illumination the incident electric field is given by

$$\mathbf{E}^{inc} = kZ_0\exp(-j\mathbf{k}^{inc}\cdot\mathbf{r})\hat{\boldsymbol{\theta}}^{inc} \tag{16}$$

while for TE illumination

$$\mathbf{E}^{inc} = kZ_0\exp(-j\mathbf{k}^{inc}\cdot\mathbf{r})\hat{\boldsymbol{\phi}}^{inc}. \tag{17}$$

In (16) and (17) $\mathbf{r}$ is the vector from the origin to any point in space and the factor of kZ_0 is inserted to simplify the analysis.

For a BOR (14) can be replaced by the equivalent pair of equations

$$\frac{j}{k}\hat{\mathbf{t}}(\mathbf{r})\cdot\oint_S\{[k^2\mathbf{K}(\mathbf{r}') + \nabla'_S(\nabla'_S\cdot\mathbf{K}(\mathbf{r}')) + J'(\nabla'_S\cdot\mathbf{K}(\mathbf{r}'))\hat{\mathbf{n}}(\mathbf{r}')]G(\mathbf{r},\mathbf{r}')$$

$$-(\nabla'_S\cdot\mathbf{K}(\mathbf{r}'))\frac{\partial G(\mathbf{r},\mathbf{r}')}{\partial n'}\hat{\mathbf{n}}(\mathbf{r}')\}dS' = \frac{\hat{\mathbf{t}}(\mathbf{r})\cdot\mathbf{E}^{inc}(\mathbf{r})}{Z_0} \tag{18a}$$

and

$$\frac{j}{k}\hat{\boldsymbol{\phi}}(\mathbf{r})\cdot\oint_S\{[k^2\mathbf{K}(\mathbf{r}') + \nabla'_S(\nabla'_S\cdot\mathbf{K}(\mathbf{r}')) + J'(\nabla'_S\cdot\mathbf{K}(\mathbf{r}'))\hat{\mathbf{n}}(\mathbf{r}')]G(\mathbf{r},\mathbf{r}')$$

$$-(\nabla'_S\cdot\mathbf{K}(\mathbf{r}'))\frac{\partial G(\mathbf{r},\mathbf{r}')}{\partial n'}\hat{\mathbf{n}}(\mathbf{r}')\}dS' = \frac{\hat{\boldsymbol{\phi}}(\mathbf{r})\cdot\mathbf{E}^{inc}(\mathbf{r})}{Z_0}. \tag{18b}$$

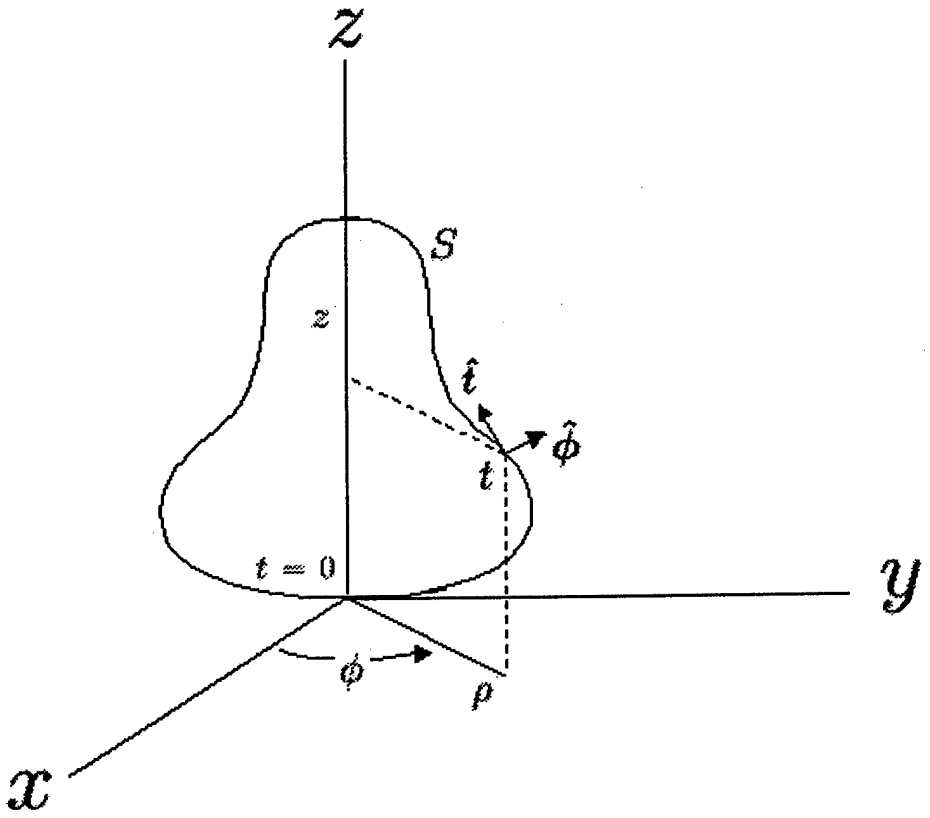

Figure 1: Body of revolution and coordinate system.

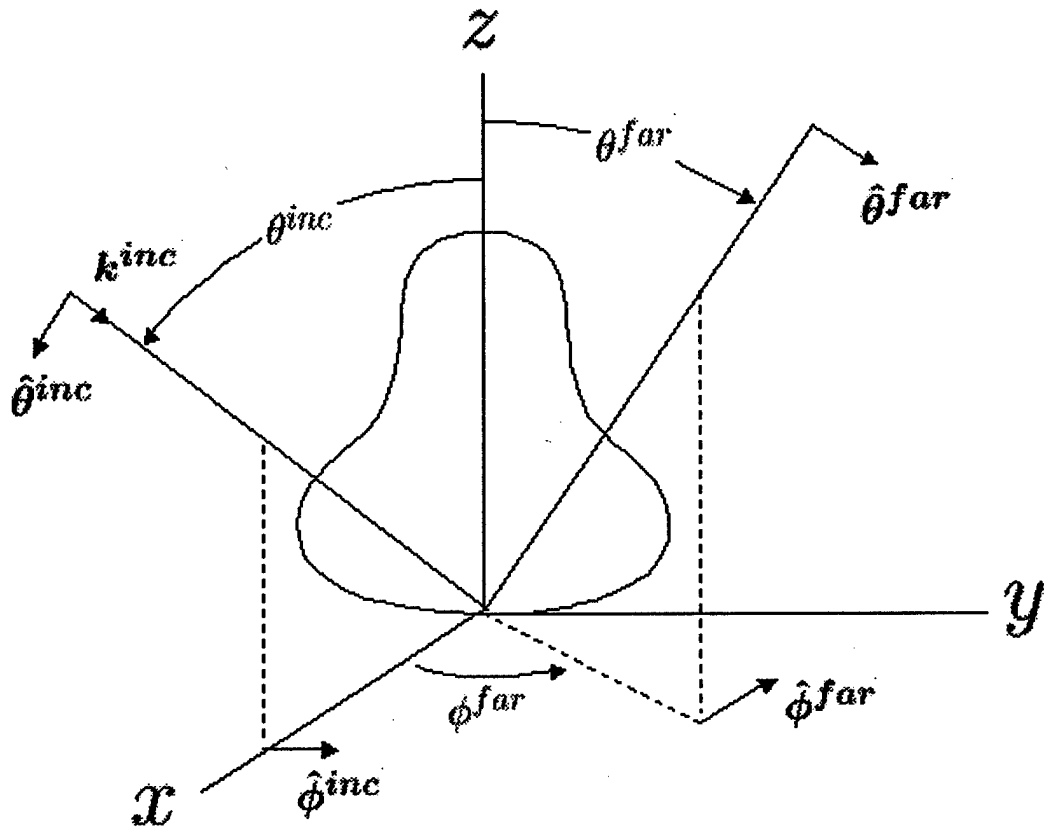

Figure 2: Plane wave scattering by a body of revolution.

The LEFIE for a PEC scatterer with a closed smooth surface in (14) and for closed smooth BORs in (18), like the original EFIE in (7), produce a unique solution for the surface current $\mathbf{K}$ except at frequencies equal to the resonant frequencies of the cavity formed by the closed surface S of the scatterer. These spurious resonances can be eliminated from the LEFIE in the same way they have been eliminated from the EFIE. For example, the LEFIE can be combined with the magnetic-field integral equation [4] or added to a corresponding LEFIE that is satisfied on a dual surface just inside the surface S of the scatterer [5]–[9]. To concentrate on the subject of lowering the order of the singularity of the EFIE and not on the details of these methods for eliminating spurious resonances, we shall choose frequencies in our numerical examples that are sufficiently far from any cavity resonance to avoid numerical instabilities.

2.3 Solution of the LEFIE by the Method of Moments

To solve the LEFIE (18) for the surface current $\mathbf{K}$ we begin by expanding $\mathbf{K}$ in a Fourier series

$$\mathbf{K}(t',\phi') = \sum_{n=-N}^{N} \left[K_n^t(t')\hat{\mathbf{t}}(t',\phi') + K_n^\phi(t')\hat{\boldsymbol{\phi}}(\phi')\right] e^{jn\phi'}. \tag{19}$$

The choice of the value of N is discussed in Section 2.8. To obtain separate integral equations for each of the Fourier modes we multiply both sides of (18a) and (18b) by $e^{-jm\phi}, m = 0, \pm 1, \pm 2, \cdots$, and integrate with respect to ϕ from $-\pi$ to π. As will be seen below, the integrands of the LHSs of (18a) and (18b) are of the form $F(t,t',\phi'-\phi)e^{jn\phi'}$, if the dot products of $\hat{\mathbf{t}}$ and $\hat{\boldsymbol{\phi}}$ are taken inside the integral signs. Noting that $dS' = \rho' dt' d\phi'$ and performing the integration with respect to ϕ' from $-\pi$ to π as well as the integration with respect to ϕ we then have

$$\int_{-\pi}^{\pi} d\phi e^{-jm\phi} \int_{-\pi}^{\pi} d\phi' e^{jn\phi'} F(t,t',\phi'-\phi) = \int_{-\pi}^{\pi} d\phi e^{j(n-m)\phi} \int_{-\pi}^{\pi} d\phi' e^{jn(\phi'-\phi)} F(t,t',\phi'-\phi)$$

$$= 2\pi\delta_{nm} \int_{-\pi}^{\pi} d\phi' e^{jn\phi'} F(t,t',\phi') \tag{20}$$

where the Kronecker delta δ_{nm} equals 0 for $m \neq n$ and equals 1 for $m = n$. The orthogonality of the Fourier modes thus enables separate integral equations to be obtained for each Fourier mode $e^{jn\phi}$.

Following the ϕ and ϕ' integrations we approximate $K_n^t(t')$ and $K_n^\phi(t')$ by pulse basis functions defined as follows. The generating curve of the BOR is parametrized in terms of t, the distance along the curve measured from the lower pole of the BOR. For each value of t, the corresponding point on the generating curve is given by $[\rho(t), z(t)]$. A set of $M+1$ points $p_1^\star, p_2^\star, \cdots, p_{M+1}^\star$, is chosen to discretize the generating curve with $p_1^\star = (\rho_1^\star, z_1^\star)$ the lower pole of the generating curve corresponding to $t = 0$, $p_{M+1}^\star = (\rho_{M+1}^\star, z_{M+1}^\star)$ the upper pole of the generating curve, and with $t_i^\star > t_{i-1}^\star$. The generating curve is approximated by straight line segments between adjacent points. The midpoints of the approximating straight

line segments are given by

$$(\rho_i, z_i) = \left(\frac{\rho_i^\star + \rho_{i+1}^\star}{2}, \frac{z_i^\star + z_{i+1}^\star}{2}\right),\ i = 1, 2, \cdots, M \tag{21}$$

and the length of the i^{th} straight line segment denoted by

$$d_i = \left[\left(\rho_{i+1}^\star - \rho_i^\star\right)^2 + \left(z_{i+1}^\star - z_i^\star\right)^2\right]^{1/2}. \tag{22}$$

For calculation purposes the discretized generating curve then completely replaces the original generating curve and the parameter t now becomes the length along the discretized curve from the lower pole instead of the length along the original generating curve from the lower pole. Thus, for example, $t(p_1^\star) = 0$, $t(p_2^\star) = d_1$, $t(p_3^\star) = d_1 + d_2$, etc. A pulse basis function $p_i(t)$ is defined as

$$p_i(t) = \begin{cases} 0, & t \le t_i^\star, t \ge t_{i+1}^\star \\ 1, & t_i^\star \le t \le t_{i+1}^\star \end{cases}. \tag{23}$$

Then

$$K_n^t(t') \approx \sum_{i=1}^{M} K_n^t(t_i') p_i(t') \tag{24a}$$

and

$$K_n^\phi(t') \approx \sum_{i=1}^{M} K_n^\phi(t_i') p_i(t'). \tag{24b}$$

A set of $2M$ equations for the $2M$ unknowns $K_n^t(t_i), K_n^\phi(t_i),\ i = 1, 2, \cdots, M$, is then obtained by using point-matching: the LHS and RHS of the integral equations for each Fourier mode are equated at $t = t_i,\ i = 1, 2, \cdots, M$. This set of $2M$ equations can be expressed in matrix form as

$$\begin{bmatrix} [Z_n^{tt}] & [Z_n^{t\phi}] \\ [Z_n^{\phi t}] & [Z_n^{\phi\phi}] \end{bmatrix} \begin{bmatrix} \mathbf{K}_n^t \\ \mathbf{K}_n^\phi \end{bmatrix} = \begin{bmatrix} \mathbf{V}_n^t \\ \mathbf{V}_n^\phi \end{bmatrix},\ n = 0, \pm 1, \pm 2, \cdots, \pm N. \tag{25}$$

In (25) the $[Z_n^{pq}]$, $p, q = t$ or ϕ, are $M \times M$ matrices obtained from the LHS's of (18a)and (18b). The index p corresponds to the external dot product factor $\hat{\mathbf{t}}$ or $\hat{\boldsymbol{\phi}}$, and the index q corresponds to the t or ϕ component of $\mathbf{K}$. The i^{th} row of $[Z_n^{pq}]$ corresponds to the value of the observation point t_i, and the j^{th} column of $[Z_n^{pq}]$ corresponds to $K_n^q(t_j)$. The i^{th} value of the $M \times 1$ vectors $\mathbf{K_n^t}$ and $\mathbf{K_n^\phi}$ equals $K_n^t(t_i)$ and $K_n^\phi(t_i)$ respectively. The vectors $\mathbf{V_n^t}$ and $\mathbf{V_n^\phi}$ on the RHS of (25) contain the values of the RHS's of (18a) and (18b), respectively, evaluated at $t = t_i,\ i = 1, 2, \cdots, M$, following multiplication by $e^{-jn\phi}$ and integration with respect to ϕ from $-\pi$ to π.

2.4 Expressions for the Elements of the Z Matrices

Detailed expressions will now be obtained for the elements of the Z matrices. The contribution of the dot product of $\hat{\mathbf{t}}$ or $\hat{\boldsymbol{\phi}}$ with each of the four terms under the integral sign in (18a) and (18a) will be considered in turn. Some useful relationships will first be established.

Letting v and v' be the angles measured positive clockwise from the positive z axis to $\hat{\mathbf{t}}$ and $\hat{\mathbf{t}}'$ respectively (see Fig. 3), it follows that

$$\hat{\mathbf{t}} = \cos v(t)\hat{\mathbf{z}} + \sin v(t)\hat{\boldsymbol{\rho}} = \sin v(t)\cos\phi\hat{\mathbf{x}} + \sin v(t)\sin\phi\hat{\mathbf{y}} + \cos v(t)\hat{\mathbf{z}} \tag{26a}$$

$$\hat{\boldsymbol{\phi}} = -\sin\phi\hat{\mathbf{x}} + \cos\phi\hat{\mathbf{y}} \tag{26b}$$

and similarly for $\hat{\mathbf{t}}'$ and $\hat{\boldsymbol{\phi}}'$; and hence that

$$\hat{\mathbf{n}}' = \hat{\boldsymbol{\phi}}' \times \hat{\mathbf{t}}' = \cos v'\cos\phi'\hat{\mathbf{x}} + \cos v'\sin\phi'\hat{\mathbf{y}} - \sin v'\hat{\mathbf{z}} \tag{26c}$$

so that

$$\hat{\mathbf{t}}\cdot\hat{\mathbf{t}}' = \sin v(t)\sin v'(t')\cos(\phi'-\phi) + \cos v(t)\cos v'(t') \tag{27a}$$

$$\hat{\mathbf{t}}\cdot\hat{\boldsymbol{\phi}}' = -\sin v(t)\sin(\phi'-\phi) \tag{27b}$$

$$\hat{\boldsymbol{\phi}}\cdot\hat{\mathbf{t}}' = \sin v'(t')\sin(\phi'-\phi) \tag{27c}$$

$$\hat{\boldsymbol{\phi}}\cdot\hat{\boldsymbol{\phi}}' = \cos(\phi'-\phi) \tag{27d}$$

$$\hat{\mathbf{t}}\cdot\hat{\mathbf{n}}' = \sin v\cos v'\cos(\phi'-\phi) - \cos v\sin v' \tag{27e}$$

and

$$\hat{\boldsymbol{\phi}}\cdot\hat{\mathbf{n}}' = \cos v'\sin(\phi'-\phi). \tag{27f}$$

It is also simple to show that

$$\begin{aligned} |\,\mathbf{r}-\mathbf{r}'\,| &= \left[\rho^2+\rho'^2-2\rho\rho'\cos(\phi'-\phi)+(z-z')^2\right]^{1/2} \\ &= \left[(\rho-\rho')^2+(z-z')^2+4\rho\rho'\sin^2(\frac{\phi'-\phi}{2})\right]^{1/2}. \end{aligned} \tag{28}$$

Now let

$$I_1^{pq} = \frac{j}{k}\int_{-\pi}^{\pi} d\phi e^{-jm\phi}\hat{\mathbf{p}}(\mathbf{r})\cdot\int_S k^2\sum_n K_n^q(t')e^{jn\phi'}\hat{\mathbf{q}}(\mathbf{r}')G(|\,\mathbf{r}-\mathbf{r}'\,|)dS'$$

$$= jk\int_{-\pi}^{\pi} d\phi e^{-jm\phi}\hat{\mathbf{p}}(\mathbf{r})\cdot\int\rho' dt'\int_{-\pi}^{\pi} d\phi'\sum_n K_n^q(t')e^{jn\phi'}\hat{\mathbf{q}}(\mathbf{r}')G(|\,\mathbf{r}-\mathbf{r}'\,|),\ p,q = t \text{ or } \phi. \tag{29}$$

where the integration with respect to t' is over the length of the generating curve of the BOR. Then, using (5),(28),(27a)-(27d), and (20) we obtain

$$I_1^{tt} = jk^2\int dt'\rho' K_n^t(t')[\sin v\sin v' G_{2,n}(\rho,\rho',z-z') + \cos v\cos v' G_{1,n}(\rho,\rho',z-z')] \tag{30a}$$

$$I_1^{\phi t} = -k^2\int dt'\rho' K_n^t(t')\sin v' G_{3,n}(\rho,\rho',z-z') \tag{30b}$$

$$I_1^{t\phi} = k^2\sin v\int dt'\rho' K_n^{\phi}(t')G_{3,n}(\rho,\rho',z-z') \tag{30c}$$

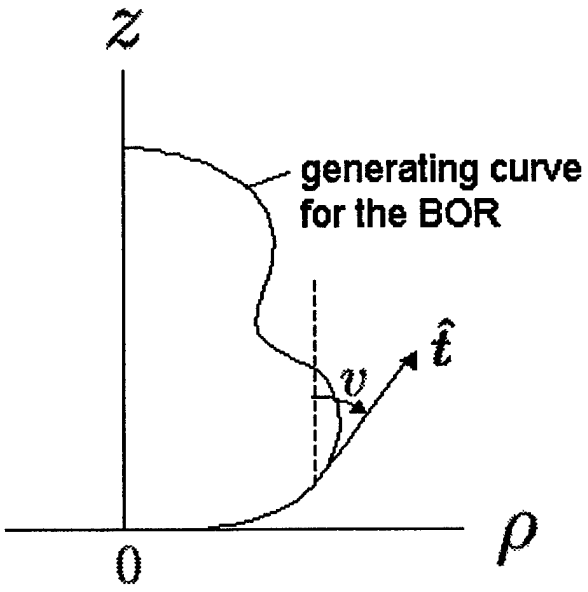

Figure 3: Defining geometry for the angle v in the ρz plane.

and

$$I_1^{\phi\phi} = jk^2 \int dt' \rho' K_n^{\phi}(t') G_{2,n}(\rho, \rho', z - z') \tag{30d}$$

where

$$G_{1,n}(\rho, \rho', z - z') = \int_0^{\pi} G_0(R) \cos(n\phi') d\phi' \tag{31a}$$

$$G_{2,n}(\rho, \rho', z - z') = \int_0^{\pi} G_0(R) \cos(n\phi') \cos\phi' d\phi' \tag{31b}$$

and

$$G_{3,n}(\rho, \rho', z - z') = \int_0^{\pi} G_0(R) \sin(n\phi') \sin\phi' d\phi' \tag{31c}$$

with

$$G_0(R) = \frac{\exp(-jkR)}{kR} \tag{31d}$$

and $R = \mid \mathbf{r} - \mathbf{r}' \mid$ given by (28). In the arguments of the $G_{k,n}, k = 1, 2, 3$, the distances ρ and z are functions of the observation point coordinate t, and ρ' and z' are functions of the source point coordinate t'.

The contributions of the I_1^{pq} to the Z_n^{pq} matrices are then (see Section 2.3)

$$[Z_n^{tt}]_{1;ij} = jk^2 d_j [\sin v_i \sin v_j G_{2,n}(\rho_i, \rho_j, z_i - z_j) + \cos v_i \cos v_j G_{1,n}(\rho_i, \rho_j, z_i - z_j)] \tag{32a}$$

$$[Z_n^{\phi t}]_{1;ij} = -k^2 d_j \rho_j \sin v_j G_{3,n}(\rho_i, \rho_j, z_i - z_j) \tag{32b}$$

$$[Z_n^{t\phi}]_{1;ij} = k^2 \sin v_i d_j \rho_j G_{3,n}(\rho_i, \rho_j, z_i - z_j) \tag{32c}$$

and

$$[Z_n^{\phi\phi}]_{1;ij} = jk^2 d_j G_{2,n}(\rho_i, \rho_j, z_i - z_j). \tag{32d}$$

In (32) the subscripts i and j indicate observation point and source point, respectively, and the discretized values of $\sin v$ and $\cos v$ are given by

$$\sin v_i = \frac{\rho_{i+1}^{\star} - \rho_i^{\star}}{d_i} \tag{33a}$$

and

$$\cos v_i = \frac{z_{i+1}^{\star} - z_i^{\star}}{d_i}. \tag{33b}$$

Next let

$$I_2^{pq} = \frac{j}{k} \int_{-\pi}^{\pi} d\phi e^{-jm\phi} \hat{\mathbf{p}}(\mathbf{r}) \cdot \int_S \nabla'_S \left[\nabla'_S \cdot \sum_n K_n^q(t') e^{jn\phi'} \hat{\mathbf{q}}(\mathbf{r}') \right] G(\mid \mathbf{r} - \mathbf{r}' \mid) dS'$$

$$= \frac{j}{k} \int_{-\pi}^{\pi} d\phi e^{-jm\phi} \hat{\mathbf{p}}(\mathbf{r}) \cdot \int \rho' dt' \int_{-\pi}^{\pi} d\phi' \nabla'_S \left[\nabla'_S \cdot \sum_n K_n^q(t') e^{jn\phi'} \hat{\mathbf{q}}(\mathbf{r}') \right] G(\mid \mathbf{r} - \mathbf{r}' \mid),$$

$$p, q = t \text{ or } \phi. \tag{34}$$

Making use of the relationships [2, Appendix 2, 73. and 74.]

$$\nabla'_S \cdot [\hat{\mathbf{t}}' K_n^t(t') e^{jn\phi'}] = \frac{1}{\rho'} \frac{d}{dt'} [\rho' K_n^t(t')] e^{jn\phi'} \tag{35a}$$

$$\nabla'_S \cdot \left[\hat{\boldsymbol{\phi}}' K_n^\phi(t') e^{jn\phi'}\right] = \frac{jn}{\rho'} K_n^\phi(t') e^{jn\phi'} \tag{35b}$$

$$\nabla'_S [\nabla'_S \cdot \hat{\mathbf{t}}' K_n^t(t') e^{jn\phi'}] = \left(\frac{d}{dt'} \frac{1}{\rho'} \frac{d}{dt'} [\rho' K_n^t(t')] \hat{\mathbf{t}}' + jn \frac{1}{\rho'^2} \frac{d}{dt'} [\rho' K_n^t(t')] \hat{\boldsymbol{\phi}}' \right) e^{jn\phi'} \tag{35c}$$

$$\nabla'_S \left[\nabla'_S \cdot \hat{\boldsymbol{\phi}}' K_n^\phi(t') e^{jn\phi'}\right] = \left(jn \frac{d}{dt'} \left[\frac{K_n^\phi(t')}{\rho'} \right] \hat{\mathbf{t}}' - \frac{n^2}{\rho'^2} K_n^\phi(t') \hat{\boldsymbol{\phi}}' \right) e^{jn\phi'} \tag{35d}$$

and (5),(28),(27a)-(27d), and (20), we obtain

$$I_2^{tt} = j \int dt' \rho' \frac{d}{dt'} \left(\frac{1}{\rho'} \frac{d}{dt'} [\rho' K_n^t(t')] \right) [\sin v \sin v' G_{2,n}(\rho, \rho', z - z') + \cos v \cos v' G_{1,n}(\rho, \rho', z - z')]$$

$$+ jn \sin v \int dt' \frac{1}{\rho'} \frac{d}{dt'} [\rho' K_n^t(t')] G_{3,n}(\rho, \rho', z - z') \tag{36a}$$

$$I_2^{\phi t} = - \int dt' \rho' \frac{d}{dt'} \left(\frac{1}{\rho'} \frac{d}{dt'} [\rho' K_n^t(t')] \right) \sin v' G_{3,n}(\rho, \rho', z - z')$$

$$- n \int dt' \frac{1}{\rho'} \frac{d'}{dt} [\rho' K_n^t(t')] G_{2,n}(\rho, \rho', z - z') \tag{36b}$$

$$I_2^{t\phi} = -n \int dt' \rho' \frac{d}{dt'} \left[\frac{K_n^\phi(t')}{\rho'} \right] [\sin v \sin v' G_{2,n}(\rho, \rho', z - z') + \cos v \cos v' G_{1,n}(\rho, \rho', z - z')]$$

$$- n^2 \sin v \int dt' \frac{K_n^\phi(t')}{\rho'} G_{3,n}(\rho, \rho', z - z') \tag{36c}$$

and

$$I_2^{\phi\phi} = -jn \int dt' \rho' \frac{d}{dt'} \left[\frac{K_n^\phi(t')}{\rho'} \right] \sin v' G_{3,n}(\rho, \rho', z - z') - jn^2 \int dt' \frac{1}{\rho'} K_n^\phi(t') G_{2,n}(\rho, \rho', z - z'). \tag{36d}$$

Before obtaining the contribution of I_2^{pq} to $[Z_n^{pq}]$ it is necessary to consider the derivatives appearing in (36). The details of the derivative approximations will be treated in Section 2.9. For our purposes here it suffices to note that a quadratic Lagrangian interpolation polynomial is used to obtain approximations for both the first and second derivatives. For the first derivatives

$$\frac{d}{dt'} \left[\rho' K_n^t(t') \right]_{t'=t_j} \approx \sum_{k=-1}^{1} c'_{j+k} \rho_{j+k} K_{n,j+k}^t \tag{37a}$$

and

$$\frac{d}{dt'} \left[\frac{1}{\rho'} K_n^\phi(t') \right]_{t'=t_j} \approx \sum_{k=-1}^{1} c'_{j+k} \frac{1}{\rho_{j+k}} K_{n,j+k}^\phi \tag{37b}$$

where we have denoted $K_n^t(t_j)$ and $K_n^\phi(t_j)$ by $K_{n,j}^t$ and $K_{n,j}^\phi$ respectively. For the second derivative

$$\frac{d^2}{dt'^2}\left[\rho' K_n^t(t')\right]_{t'=t_j} \approx \sum_{k=-1}^{1} c''_{j+k}\rho_{j+k}K_{n,j+k}^t. \tag{38}$$

Since

$$\frac{d}{dt'}\left(\frac{1}{\rho'}\frac{d}{dt'}\left[\rho' K_n^t(t')\right]\right) = \frac{1}{\rho'}\frac{d^2}{dt'^2}\left[\rho' K_n^t(t')\right] - \frac{1}{\rho'^2}\frac{d\rho'}{dt'}\frac{d}{dt'}\left[\rho' K_n^t(t')\right] \tag{39}$$

$$\frac{d}{dt'}\left(\frac{1}{\rho'}\frac{d}{dt'}\left[\rho' K_n^t(t')\right]\right)_{t'=t_j} \approx \frac{1}{\rho_j}\sum_{k=-1}^{1} c''_{j+k}\rho_{j+k}K_{n,j+k}^t - \frac{1}{\rho_j^2}\sin v_j \sum_{k=-1}^{1} c'_{j+k}\rho_{j+k}K_{n,j+k}^t \tag{40}$$

where we have used (33) to approximate dp'/dt'. In (37),(38), and (40), when $j = 1$, k is summed from 0 to 2, and when $j = M$, k is summed from -2 to 0. Using the derivative approximations (37), and (40) we then obtain the following contributions of the I_2^{pq} to the Z_n^{pq} matrices:

$$[Z_n^{tt}]_{2;i,j+k} = jd_j\rho_j\left[\sin v_i \sin v_j G_{2,n}(\rho_i,\rho_j,z_i-z_j) + \cos v_i \cos v_j G_{1,n}(\rho_i,\rho_j,z_i-z_j)\right]$$

$$\cdot\left(\frac{1}{\rho_j}c''_{j+k}\rho_{j+k} - \frac{1}{\rho_j^2}\sin v_j c'_{j+k}\rho_{j+k}\right) + jn\sin v_i d_j G_{3,n}(\rho_i,\rho_j,z_i-z_j)\frac{1}{\rho_j^2}c''_{j+k}\rho_{j+k} \tag{41a}$$

$$[Z_n^{\phi t}]_{2;i,j+k} = -d_j\rho_j \sin v_j G_{3,n}(\rho_i,\rho_j,z_i-z_j)\left(\frac{1}{\rho_j}c''_{j+k}\rho_{j+k} - \frac{1}{\rho_j^2}\sin v_j c'_{j+k}\rho_{j+k}\right)$$

$$-nd_j G_{2,n}(\rho_i,\rho_j,z_i-z_j)c'_{j+k}\rho_{j+k} \tag{41b}$$

$$[Z_n^{t\phi}]_{2;i,j+k} = -nd_j\rho_j\left[\sin v_i \sin v_j G_{2,n}(\rho_i,\rho_j,z_i-z_j) + \cos v_i \cos v_j G_{1,n}(\rho_i,\rho_j,z_i-z_j)\right]c'_{j+k}\frac{1}{\rho_{j+k}}$$

$$-n^2 \sin v_i d_j \frac{1}{\rho_j}G_{3,n}(\rho_i,\rho_j,z_i-z_j)\mid_{k=0} \tag{41c}$$

and

$$[Z_n^{\phi\phi}]_{2;i,j} = -jnd_j\rho_j \sin v_j G_{3,n}(\rho_i,\rho_j,z_i-z_j) - jn^2\frac{d_j}{\rho_j}G_{2,n}(\rho_i,\rho_j,z_i-z_j). \tag{41d}$$

The index k in these expressions takes the values $-1, 0, 1$ for $j = 2, 3, \cdots, M-1$, and the values $0, 1, 2$ and $-2, -1, 0$ for $j = 1$ and $j = M$, respectively.

Next let

$$I_3^{pq} = \frac{j}{k}\int_{-\pi}^{\pi} d\phi e^{-jm\phi}\hat{\mathbf{p}}(\mathbf{r})\cdot\int_S J'\nabla'_S\cdot\left[\hat{\mathbf{q}}(\mathbf{r}')\sum_n K_n^q(t')e^{jn\phi'}\right]\hat{\mathbf{n}}(\mathbf{r}')G(\mid\mathbf{r}-\mathbf{r}'\mid)dS'$$

$$= \frac{j}{k}\int_{-\pi}^{\pi} d\phi e^{-jm\phi}\hat{\mathbf{p}}(\mathbf{r})\cdot\int\rho' J'(t')dt'\int_{-\pi}^{\pi} d\phi'\nabla'_S\cdot\left[\hat{\mathbf{q}}(\mathbf{r}')\sum_n K_n^q(t')e^{jn\phi'}\right]\hat{\mathbf{n}}(\mathbf{r}')G(\mid\mathbf{r}-\mathbf{r}'\mid),$$

$$p, q = t \text{ or } \phi. \tag{42}$$

Using (35a),(35b),(5),(28),(27e),(27f), and (20) we obtain

$$I_3^{tt} = j\int dt' \frac{d}{dt'}[\rho' K_n^t(t')]J(t')\,[\sin v\cos v' G_{2,n}(\rho,\rho',z-z') - \cos v \sin v' G_{1,n}(\rho,\rho',z-z')] \tag{43a}$$

$$I_3^{\phi t} = -\int dt' \frac{d}{dt'}[\rho' K_n^t(t')]J(t')\cos v' G_{3,n}(\rho,\rho',z-z') \tag{43b}$$

$$I_3^{t\phi} = -n\int dt' K_n^{\phi}(t')J(t')\,[\sin v\cos v' G_{2,n}(\rho,\rho',z-z') - \cos v \sin v' G_{1,n}(\rho,\rho',z-z')] \tag{43c}$$

and

$$I_3^{\phi\phi} = -jn\int dt' K_n^{\phi}(t')J(t')\cos v' G_{3,n}(\rho,\rho',z-z'). \tag{43d}$$

Using the first derivative approximation (37) the corresponding contributions to the Z_n^{pq} matrices are then

$$[Z_n^{tt}]_{3;i,j+k} = jd_j J(t_j)[\sin v_i \cos v_j G_{2,n}(\rho_i,\rho_j,z_i-z_j)$$

$$-\cos v_i \sin v_j G_{1,n}(\rho_i,\rho_j,z_i-z_j)]c'_{j+k}\rho_{j+k} \tag{44a}$$

$$[Z_n^{\phi t}]_{3;i,j+k} = -d_j J(t_j)\cos v_j G_{3,n}(\rho_i,\rho_j,z_i-z_j)c'_{j+k}\rho_{j+k} \tag{44b}$$

$$[Z_n^{t\phi}]_{3;i,j} = -nd_j J(t_j)[\sin v_i \cos v_j G_{2,n}(\rho_i,\rho_j,z_i-z_j) - \cos v_i \sin v_j G_{1,n}(\rho_i,\rho_j,z_i-z_j)] \tag{44c}$$

and

$$[Z_n^{\phi\phi}]_{3;i,j} = -jnd_j J(t_j)\cos v_j G_{3,n}(\rho_i,\rho_j,z_i-z_j). \tag{44d}$$

Finally let

$$I_4^{pq} = -\frac{j}{k}\int_{-\pi}^{\pi} d\phi e^{-jm\phi}\hat{\mathbf{p}}(\mathbf{r})\cdot\int_S \nabla'_S\cdot\left[\hat{\mathbf{q}}(\mathbf{r}')\sum_n K_n^q(t')e^{jn\phi'}\right]\frac{\partial G(|\,\mathbf{r}-\mathbf{r}'\,|)}{\partial n'}\hat{\mathbf{n}}(\mathbf{r}')dS'$$

$$= -\frac{j}{k}\int_{-\pi}^{\pi} d\phi e^{-jm\phi}\hat{\mathbf{p}}(\mathbf{r})\cdot\int \rho' dt'\int_{-\pi}^{\pi} d\phi'\nabla'_S\cdot[\hat{\mathbf{q}}(\mathbf{r}')\sum_n K_n^q(t')e^{jn\phi'}]\frac{\partial G(|\,\mathbf{r}-\mathbf{r}'\,|)}{\partial n'}\hat{\mathbf{n}}(\mathbf{r}'),$$

$$p,q = t \text{ or } \phi. \tag{45}$$

Using (33),(5),(28),(27e),(27f),(20), (26c), and noting that

$$\frac{\partial G(|\,\mathbf{r}-\mathbf{r}'\,|)}{\partial n'} = \nabla' G(|\,\mathbf{r}-\mathbf{r}'\,|)\cdot\hat{\mathbf{n}}(\mathbf{r}') \tag{46}$$

$$\nabla' G(|\,\mathbf{r}-\mathbf{r}'\,|) = \frac{1}{4\pi}\frac{jkR+1}{R^3}e^{-jkR}(\mathbf{r}-\mathbf{r}'),\quad R = \mathbf{r}-\mathbf{r}' \tag{47}$$

we obtain

$$I_4^{tt} = -jk^2\int dt' \frac{d}{dt'}[\rho' K_n^t(t')][\rho\sin v\cos^2 v' H_{4,n}(\rho,\rho',z-z') - \rho\cos v\cos v'\sin v' H_{2,n}(\rho,\rho',z-z')$$

$$-\sin v\rho'\cos^2 v' H_{2,n}(\rho,\rho',z-z') + \cos v\rho'\cos v'\sin v' H_{1,n}(\rho,\rho',z-z')$$

$$-(z-z')\sin v\cos v'\sin v' H_{2,n}(\rho,\rho',z-z') + \cos v(z-z')\sin^2 v' H_{1,n}(\rho,\rho',z-z')] \tag{48a}$$

$$I_4^{\phi t} = k^2 \int dt' \frac{d}{dt'}[\rho' K_n^t(t')][\rho \cos^2 v' H_{5,n}(\rho, \rho', z - z') - \rho \cos^2 v' H_{3,n}(\rho, \rho', z - z')$$
$$-(z - z') \cos v' \sin v' H_{3,n}(\rho, \rho', z - z')] \tag{48b}$$

$$I_4^{t\phi} = nk^2 \int dt' K_n^{\phi}(t')[\rho \sin v \cos^2 v' H_{4,n}(\rho, \rho', z - z') - \rho \cos v \cos v' \sin v' H_{2,n}(\rho, \rho', z - z')$$
$$- \sin v \rho' \cos^2 v' H_{2,n}(\rho, \rho', z - z') + \cos v \rho' \cos v' \sin v' H_{1,n}(\rho, \rho', z - z')$$
$$-(z - z') \sin v \cos v' \sin v' H_{2,n}(\rho, \rho', z - z') + \cos v (z - z') \sin^2 v' H_{1,n}(\rho, \rho', z - z')] \tag{48c}$$

and

$$I_4^{\phi\phi} = jk^2 n \int dt' K_n^{\phi}(t')[\rho \cos^2 v' H_{5,n}(\rho, \rho', z - z') - \rho \cos^2 v' H_{3,n}(\rho, \rho', z - z')$$
$$-(z - z') \cos v' \sin v' H_{3,n}(\rho, \rho', z - z')]. \tag{48d}$$

In (48)

$$H_{1,n}(\rho, \rho', z - z') = \int_0^{\pi} H_0(R) \cos(n\phi') d\phi' \tag{49a}$$

$$H_{2,n}(\rho, \rho', z - z') = \int_0^{\pi} H_0(R) \cos(n\phi') \cos\phi' d\phi' \tag{49b}$$

$$H_{3,n}(\rho, \rho', z - z') = \int_0^{\pi} H_0(R) \sin(n\phi') \sin\phi' d\phi' \tag{49c}$$

$$H_{4,n}(\rho, \rho', z - z') = \int_0^{\pi} H_0(R) \cos(n\phi') \cos^2\phi' d\phi' \tag{49d}$$

$$H_{5,n}(\rho, \rho', z - z') = \int_0^{\pi} H_0(R) \sin(n\phi') \cos\phi' \sin\phi' d\phi' \tag{49e}$$

with

$$H_0(R) = \frac{1 + jkR}{(kR)^3} \exp(-jkR) \tag{49f}$$

and $R = |\, \mathbf{r} - \mathbf{r}' \,|$ given by (28). Using the first derivative approximation (37) the corresponding contributions to the Z_n^{pq} matrices are then

$$[Z_n^{tt}]_{4;i,j+k} = -jk^2 d_j[\rho_i \sin v_i \cos^2 v_j H_{4,n}(\rho_i, \rho_j, z_i - z_j) - \rho_i \cos v_i \cos v_j \sin v_j H_{2,n}(\rho_i, \rho_j, z_i - z_j)$$
$$- \sin v_i \rho_j \cos^2 v_j H_{2,n}(\rho_i, \rho_j, z_i - z_j) + \cos v_i \rho_j \cos v_j \sin v_j H_{1,n}(\rho_i, \rho_j, z_i - z_j)$$
$$-(z_i - z_j) \sin v_i \cos v_j \sin v_j H_{2,n}(\rho_i, \rho_j, z_i - z_j)$$
$$+ \cos v_i (z_i - z_j) \sin^2 v_j H_{1,n}(\rho_i, \rho_j, z_i - z_j)] c'_{j+k} \rho_{j+k} \tag{50a}$$

$$[Z_n^{\phi t}]_{4;i,j+k} = k^2 d_j[\rho_i \cos^2 v_j H_{5,n}(\rho_i, \rho_j, z_i - z_j) - \rho_i \cos^2 v_j H_{3,n}(\rho_i, \rho_j, z_i - z_j)$$
$$-(z - z') \cos v_j \sin v_j H_{3,n}(\rho_i, \rho_j, z_i - z_j)] c'_{j+k} \rho_{j+k} \tag{50b}$$

$$[Z_n^{t\phi}]_{4;i,j} = nk^2 d_j[\rho_i \sin v_i \cos^2 v_j H_{4,n}(\rho_i, \rho_j, z_i - z_j) - \rho_i \cos v_i \cos v_j \sin v_j H_{2,n}(\rho_i, \rho_j, z_i - z_j)$$
$$- \sin v_i \rho_j \cos^2 v_j H_{2,n}(\rho_i, \rho_j, z_i - z_j) + \cos v_i \rho_j \cos v_j \sin v_j H_{1,n}(\rho_i, \rho_j, z_i - z_j)$$
$$-(z_i - z_j) \sin v_i \cos v_j \sin v_j H_{2,n}(\rho_i, \rho_j, z_i - z_j) + \cos v_i (z_i - z_j) \sin^2 v_j H_{1,n}(\rho_i, \rho_j, z_i - z_j)] \quad (50c)$$

and

$$[Z_n^{\phi\phi}]_{i,j} = jk^2 n d_j[\rho_i \cos^2 v_j H_{5,n}(\rho_i, \rho_j, z_i - z_j) - \rho_i \cos^2 v_j H_{3,n}(\rho_i, \rho_j, z_i - z_j)$$
$$-(z_i - z_j) \cos v_j \sin v_j H_{3,n}(\rho_i, \rho_j, z_i - z_j). \quad (50d)$$

Equations (32), (41), (44), and (50) give the contributions of the four terms under the integral sign of (18) to the Z_n^{pq} matrices in (25) so that

$$[Z_n^{pq}] = [Z_n^{pq}]_1 + [Z_n^{pq}]_2 + [Z_n^{pq}]_3 + [Z_n^{pq}]_4, \quad p, q = t \text{ or } \phi. \quad (51)$$

It is easy to see from (31), (49), (32), (41), (44) and (50) that

$$[Z_{-n}^{tt}] = [Z_n^{tt}] \quad (52a)$$

$$[Z_{-n}^{t\phi}] = -[Z_n^{t\phi}] \quad (52b)$$

$$[Z_{-n}^{\phi t}] = -[Z_n^{\phi t}] \quad (52c)$$

and

$$[Z_{-n}^{\phi\phi}] = [Z_n^{\phi\phi}]. \quad (52d)$$

2.5 Expressions for the Elements of the V Vectors

Now that we have obtained detailed expressions for the elements of the Z matrices we turn to the elements of the column vectors $\mathbf{V}_n^t$ and $\mathbf{V}_n^\phi$ in (25). Recall that the V vectors represent the RHS's of (18) multiplied by $\exp(-jn\phi)$ and integrated with respect to ϕ from $-\pi$ to π and evaluated at the M points $t = t_i,\ i = 1, 2, \cdots, M$, and that the incident electric field is given by (16) and (17) for TM and TE polarization, respectively. Then

$$V_{ni}^{pq} = \frac{1}{Z_0} \int_{-\pi}^{\pi} d\phi e^{-jn\phi} \hat{\mathbf{p}}(t_i, \phi) \cdot kZ_0 \exp[\mathbf{k}^{inc} \cdot \mathbf{r}(t_i, \phi)] \hat{\mathbf{q}}^{inc}, \quad p = t \text{ or } \phi,\ q = \theta \text{ or } \phi. \quad (53)$$

Using (26a) and (26b) it is simple to establish the unit vector relations

$$\hat{\mathbf{t}} \cdot \hat{\boldsymbol{\theta}}^{inc} = \cos\theta^{inc} \sin v(t) \cos(\phi - \phi^{inc}) - \sin\theta^{inc} \cos v(t) \quad (54a)$$

$$\hat{\boldsymbol{\phi}} \cdot \hat{\boldsymbol{\theta}}^{inc} = -\cos\theta^{inc} \sin(\phi - \phi^{inc}) \quad (54b)$$

$$\hat{\mathbf{t}} \cdot \hat{\boldsymbol{\phi}}^{inc} = \sin v(t) \sin(\phi - \phi^{inc}) \quad (54c)$$

and

$$\hat{\boldsymbol{\phi}} \cdot \hat{\boldsymbol{\phi}}^{inc} = \cos(\phi - \phi^{inc}). \quad (54d)$$

Also, using (15)

$$\mathbf{k}^{inc} \cdot \mathbf{r}(t_i, \phi) = -k(\sin\theta^{inc}\hat{\mathbf{x}} + \cos\theta^{inc}\hat{\mathbf{z}}) \cdot (\rho_i \cos\phi\hat{\mathbf{x}} + \rho_i \sin\phi\hat{\mathbf{y}} + z_i\hat{\mathbf{z}})$$

$$= -k\rho_i \sin\theta^{inc}\cos\phi - kz_i\cos\theta^{inc} \tag{55}$$

where as in Section 2.3 we have let $\rho_i = \rho(t_i)$ and $z_i = z(t_i)$. Hence, recalling that it has been assumed that $\phi^{inc} = 0$, we then obtain from (53)

$$V_{ni}^{t\theta} = ke^{jkz_i\cos\theta^{inc}}\Big[\cos\theta^{inc}\sin v_i\int_0^{2\pi} d\phi\cos\phi e^{j(k\rho_i\sin\theta^{inc}\cos\phi - n\phi)}$$

$$-\sin\theta^{inc}\cos v_i\int_0^{2\pi} d\phi e^{j(k\rho_i\sin\theta^{inc}\cos\phi - n\phi)}\Big] \tag{56a}$$

$$V_{ni}^{\phi\theta} = -\cos\theta^{inc}ke^{jkz_i\cos\theta^{inc}}\int_0^{2\pi} d\phi\sin\phi e^{j(k\rho_i\sin\theta^{inc}\cos\phi - n\phi)} \tag{56b}$$

$$V_{ni}^{t\phi} = ke^{jkz_i\cos\theta^{inc}}\sin v_i\int_0^{2\pi} d\phi\sin\phi e^{j(k\rho_i\sin\theta^{inc}\cos\phi - n\phi)} \tag{56c}$$

and

$$V_{ni}^{\phi\phi} = ke^{jkz_i\cos\theta^{inc}}\int_0^{2\pi} d\phi\cos\phi e^{j(k\rho_i\sin\theta^{inc}\cos\phi - n\phi)}, \tag{56d}$$

where we have changed the limits of the ϕ integration to 0 to 2π. Using the integral representation for the Bessel function

$$J_n(x) = \frac{j^{-n}}{2\pi}\int_0^{2\pi} e^{j(x\cos\phi - n\phi)}d\phi \tag{57}$$

it is simple to obtain the integral representations

$$\int_0^{2\pi}\sin\phi e^{j(x\cos\phi - n\phi)}d\phi = -\pi j^n[J_{n+1}(x) + J_{n-1}(x)] \tag{58a}$$

and

$$\int_0^{2\pi}\cos\phi e^{j(x\cos\phi - n\phi)}d\phi = \pi j^{n+1}[J_{n+1}(x) - J_{n-1}(x)] \tag{58b}$$

so that

$$V_{ni}^{t\theta} = \pi j^{n+1}k\left[\cos\theta^{inc}\sin v_i(J_{n+1} - J_{n-1}) + 2j\sin\theta^{inc}\cos v_i J_n\right]e^{jkz_i\cos\theta^{inc}} \tag{59a}$$

$$V_{ni}^{\phi\theta} = \pi j^n k\cos\theta^{inc}(J_{n+1} + J_{n-1})e^{jkz_i\cos\theta^{inc}} \tag{59b}$$

$$V_{ni}^{t\phi} = -\pi j^n k\sin v_i(J_{n+1} + J_{n-1})e^{jkz_i\cos\theta^{inc}} \tag{59c}$$

and

$$V_{ni}^{\phi\phi} = \pi j^{n+1}k(J_{n+1} - J_{n-1})e^{jkz_i\cos\theta^{inc}} \tag{59d}$$

where we have let

$$J_n = J_n(k\rho_i \sin\theta^{inc}). \tag{59e}$$

Using the Bessel function relation

$$J_{-n}(z) = (-1)^n J_n(z) \tag{60}$$

it is easy to show from (59) that

$$V_{-ni}^{t\theta} = V_{ni}^{t\theta} \tag{61a}$$

$$V_{-ni}^{\phi\theta} = -V_{ni}^{\phi\theta} \tag{61b}$$

$$V_{-ni}^{t\phi} = -V_{ni}^{t\phi} \tag{61c}$$

and

$$V_{-ni}^{\phi\phi} = V_{ni}^{\phi\phi}. \tag{61d}$$

2.6 Calculation of the Current

To calculate the current on the BOR surface we refer to (19) and (24) and write

$$\mathbf{K}^q(t,\phi) = \sum_{n=-N}^{N} e^{jn\phi} \sum_i \left[K_{ni}^{tq} p_i(t)\hat{\mathbf{t}}(t,\phi) + K_{ni}^{\phi q} p_i(t)\hat{\boldsymbol{\phi}}(\phi) \right] \tag{62}$$

where $q = \theta$ (TM) or ϕ (TE) indicates the polarization of the incident electric field given by (16) or (17), and $(K_{ni}^{tq}, K_{ni}^{\phi q})$ are the elements of the vectors $(\mathbf{K}_n^{tq}, \mathbf{K}_n^{\phi q})$, obtained as the solution of the matrix equation (see (25))

$$\begin{bmatrix} [Z_n^{tt}] & [Z_n^{t\phi}] \\ [Z_n^{\phi t}] & [Z_n^{\phi\phi}] \end{bmatrix} \begin{bmatrix} \mathbf{K}_n^{tq} \\ \mathbf{K}_n^{\phi q} \end{bmatrix} = \begin{bmatrix} \mathbf{V}_n^{tq} \\ \mathbf{V}_n^{\phi q} \end{bmatrix}, \; n = 0, \pm 1, \pm 2, \cdots, \pm N. \tag{63}$$

Letting $\tilde{p} = [p_1(t), p_2(t), \cdots p_N(t)]$ be the row vector of the pulse basis functions $p_i(t)$ defined by (23) (we use the tilde to indicate the transpose of a column vector), (62) can be written as

$$\mathbf{K}^q(t,\phi) = \sum_{n=-N}^{N} e^{jn\phi} \left[\tilde{p}\mathbf{K}_n^{tq}\hat{\mathbf{t}}(t,\phi) + \tilde{p}\mathbf{K}_n^{\phi q}\hat{\boldsymbol{\phi}}(\phi) \right]. \tag{64}$$

From (63), the relations (57) for the Z_{-n} matrices in terms of the Z_n matrices, and the relations (61) for the V_{-n} vectors in terms of the V_n vectors, it is simple to derive the relations

$$\mathbf{K}_{-n}^{t\theta} = \mathbf{K}_n^{t\theta} \tag{65a}$$

$$\mathbf{K}_{-n}^{\phi\theta} = -\mathbf{K}_n^{\phi\theta} \tag{65b}$$

$$\mathbf{K}_{-n}^{t\phi} = -\mathbf{K}_n^{t\phi} \tag{65c}$$

and

$$\mathbf{K}_{-n}^{\phi\phi} = \mathbf{K}_n^{\phi\phi}. \tag{65d}$$

(Note that (65b) and (65c) imply that $\mathbf{K}_0^{\phi\theta} = 0$ and $\mathbf{K}_0^{t\phi} = 0$.) Substituting (65) in (64) then yields the expressions for the currents induced on the surface of the BOR by a TM and TE linearly polarized incident plane wave, respectively:

$$\mathbf{K}^{\theta}(t,\phi) = \tilde{p}\mathbf{K}_0^{t\theta}\hat{\mathbf{t}}(t,\phi) + 2\sum_{n=1}^{N}\left[(\tilde{p}\mathbf{K}_n^{t\theta})\cos n\phi\hat{\mathbf{t}} + j(\tilde{p}\mathbf{K}_n^{\phi\theta})\sin n\phi\hat{\boldsymbol{\phi}}(\phi)\right] \tag{66a}$$

and

$$\mathbf{K}^{\phi}(t,\phi) = \tilde{p}\mathbf{K}_0^{\phi\phi}\hat{\boldsymbol{\phi}} + 2\sum_{n=1}^{N}\left[(\tilde{p}\mathbf{K}_n^{t\phi})\sin n\phi\hat{\mathbf{t}}(t,\phi) + (\tilde{p}\mathbf{K}_n^{\phi\phi})\cos n\phi\hat{\boldsymbol{\phi}}(\phi)\right]. \tag{66b}$$

2.7 Calculation of the Far Scattered Field

In the far-field region the θ and ϕ components of the scattered electric field can be obtained from the vector potential $\mathbf{A}$ [10, p. 281]

$$\mathbf{E}^{sc}(\mathbf{r}) \overset{r\to\infty}{\sim} -j\omega\mathbf{A}(\mathbf{r}). \tag{67}$$

Then with (3) and (5),

$$E^{sc,pq}(\mathbf{r}) \overset{r\to\infty}{\sim} -jkZ_0\int_S [\mathbf{K}^q(\mathbf{r}')\cdot\hat{\mathbf{p}}]\frac{e^{-jk|\mathbf{r}-\mathbf{r}'|}}{4\pi\mid\mathbf{r}-\mathbf{r}'\mid}dS' \tag{68}$$

where p : θ or ϕ, indicates the far scattered field component; $\hat{\mathbf{p}}$: $\hat{\boldsymbol{\theta}}^{far}$ or $\hat{\boldsymbol{\phi}}^{far}$, is the corresponding unit vector (see Fig. 2); q : θ or ϕ, indicates the polarization, θ (TM) or ϕ (TE) of the incident electric field; $\mathbf{K}^q$ is given by (64), $\mathbf{r} = (r,\theta^{far},\phi^{far})$ is the far-field observation point, and $\mathbf{r}' = (\rho',\phi',z')$ is the source point on the BOR surface. In the far field, $\mid\mathbf{r}-\mathbf{r}'\mid$ in the phase of the Green's function can be approximated by

$$\mid\mathbf{r}-\mathbf{r}'\mid \overset{r\to\infty}{\sim} r - \rho'\sin\theta^{far}\cos(\phi'-\phi^{far}) - z'\cos\theta^{far} \tag{69}$$

so that

$$E^{sc,pq}(\mathbf{r}) \overset{r\to\infty}{\sim} -jkZ_0\frac{e^{-jkr}}{4\pi r}\int_S [\mathbf{K}^q(\mathbf{r}')\cdot\hat{\mathbf{p}}]e^{jk\rho'\sin\theta^{far}\cos(\phi'-\phi^{far})}e^{jkz'\cos\theta^{far}}dS'. \tag{70}$$

The relations (54) can be used directly to obtain

$$\hat{\mathbf{t}}'\cdot\hat{\boldsymbol{\theta}}^{far} = \cos\theta^{far}\sin v(t')\cos(\phi'-\phi^{far}) - \sin\theta^{far}\cos v(t') \tag{71a}$$

$$\hat{\boldsymbol{\phi}}'\cdot\hat{\boldsymbol{\theta}}^{far} = -\cos\theta^{far}\sin(\phi'-\phi^{far}) \tag{71b}$$

$$\hat{\mathbf{t}}'\cdot\hat{\boldsymbol{\phi}}^{far} = \sin v(t')\sin(\phi'-\phi^{far}) \tag{71c}$$

and

$$\hat{\boldsymbol{\phi}}'\cdot\hat{\boldsymbol{\phi}}^{far} = \cos(\phi'-\phi^{far}). \tag{71d}$$

Letting the elements of the vectors $\mathbf{R}_n^{tp}$ and $\mathbf{R}_n^{\phi p}$ be defined by

$$R_{ni}^{tp} = k \int_S p_i(t')(\hat{\mathbf{t}}' \cdot \hat{\mathbf{p}}) e^{jk[\rho' \sin\theta^{far} \cos(\phi' - \phi^{far}) + z' \cos\theta^{far}]} e^{jn(\phi' - \phi^{far})} dS' \tag{72a}$$

and

$$R_{ni}^{\phi p} = k \int_S p_i(t')(\hat{\boldsymbol{\phi}}' \cdot \hat{\mathbf{p}}) e^{jk[\rho' \sin\theta^{far} \cos(\phi' - \phi^{far}) + z' \cos\theta^{far}]} e^{jn(\phi' - \phi^{far})} dS' \tag{72b}$$

with $p = \theta$ or ϕ, (70) together with (64) can be written as

$$E^{sc,pq}(\mathbf{r}) \overset{r\to\infty}{\sim} \frac{-jkZ_0 e^{-jkr}}{4\pi kr} \sum_{n=-N}^{N} e^{jn\phi^{far}} \left(\tilde{\mathbf{R}}_n^{tp} \mathbf{K}_n^{tq} + \tilde{\mathbf{R}}_n^{\phi p} \mathbf{K}_n^{\phi q} \right) \tag{73}$$

where, using (72) and the 2π periodicity of the ϕ' integration

$$R_{ni}^{t\theta} = k \int dt' \rho' p_i(t') e^{jkz' \cos\theta^{far}} \Big[\cos\theta^{far} \sin v(t') \int_0^{2\pi} d\phi' \cos\phi' e^{j(k\rho' \sin\theta^{far} \cos\phi' + n\phi')}$$

$$- \sin\theta^{far} \cos v(t') \int_0^{2\pi} d\phi' e^{j(k\rho' \sin\theta^{far} \cos\phi' + n\phi')} \Big] \tag{74a}$$

$$R_{ni}^{\phi\theta} = -\cos\theta^{far} k \int dt' \rho' p_i(t') e^{jkz' \cos\theta^{far}} \int_0^{2\pi} d\phi' \sin\phi' e^{j(k\rho' \sin\theta^{far} \cos\phi' + n\phi')} \tag{74b}$$

$$R_{ni}^{t\phi} = k \int dt' \rho' p_i(t') e^{jkz' \cos\theta^{far}} \sin v(t') \int_0^{2\pi} d\phi' \sin\phi' e^{j(k\rho' \sin\theta^{far} \cos\phi' + n\phi')} \tag{74c}$$

and

$$R_{ni}^{\phi\phi} = k \int dt' \rho' p_i(t') e^{jkz' \cos\theta^{far}} \int_0^{2\pi} d\phi' \cos\phi' e^{j(k\rho' \sin\theta^{far} \cos\phi' + n\phi')}. \tag{74d}$$

Comparing (74) with (56), replacing θ^{inc} of (56) by θ^{far} and $-n$ of (56) with n, and using the definition of the pulse basis functions, we then obtain

$$R_{ni}^{t\theta} = \pi j^{n+1} k d_i \rho_i \left[\cos\theta^{far} \sin v_i (J_{n+1} - J_{n-1}) + 2j \sin\theta^{far} \cos v_i J_n \right] e^{jkz_i \cos\theta^{far}} \tag{75a}$$

$$R_{ni}^{\phi\theta} = -\pi j^n k d_i \rho_i \cos\theta^{far} (J_{n+1} + J_{n-1}) e^{jkz_i \cos\theta^{far}}, \tag{75b}$$

$$R_{ni}^{t\phi} = \pi j^n k d_i \rho_i \sin v_i (J_{n+1} + J_{n-1}) e^{jkz_i \cos\theta^{far}} \tag{75c}$$

and

$$R_{ni}^{\phi\phi} = \pi j^{n+1} k d_i \rho_i (J_{n+1} - J_{n-1}) e^{jkz_i \cos\theta^{far}} \tag{75d}$$

where

$$J_n = J_n(k\rho_i \sin\theta^{far}). \tag{75e}$$

The relations (61) apply to the R_{ni}^{pq} as well, so that

$$R_{-ni}^{t\theta} = R_{ni}^{t\theta} \tag{76a}$$

$$R_{-ni}^{\phi\theta} = -R_{ni}^{\phi\theta} \tag{76b}$$

$$R_{-ni}^{t\phi} = -R_{ni}^{t\phi} \tag{76c}$$

and

$$R_{-ni}^{\phi\phi} = R_{ni}^{\phi\phi}. \tag{76d}$$

Then, substituting (76) and (65) in (73) it is straightforward to obtain

$$E^{sc,\theta\theta}(\mathbf{r}) \overset{r\to\infty}{\sim} -\frac{jkZ_0e^{-jkr}}{4\pi kr}\left[\tilde{\mathbf{R}}_0^{t\theta}\mathbf{K}_0^{t\theta} + 2\sum_{n=1}^{N}\left(\tilde{\mathbf{R}}_n^{t\theta}\mathbf{K}_n^{t\theta} + \tilde{\mathbf{R}}_n^{\phi\theta}\mathbf{K}_n^{\phi\theta}\right)\cos(n\phi^{far})\right] \tag{77a}$$

$$E^{sc,\phi\theta}(\mathbf{r}) \overset{r\to\infty}{\sim} \frac{kZ_0e^{-jkr}}{4\pi kr}2\sum_{n=1}^{N}\left(\tilde{\mathbf{R}}_n^{t\phi}\mathbf{K}_n^{t\theta} + \tilde{\mathbf{R}}_n^{\phi\phi}\mathbf{K}_n^{\phi\theta}\right)\sin(n\phi^{far}) \tag{77b}$$

$$E^{sc,\theta\phi}(\mathbf{r}) \overset{r\to\infty}{\sim} \frac{kZ_0e^{-jkr}}{4\pi kr}2\sum_{n=1}^{N}\left(\tilde{\mathbf{R}}_n^{t\theta}\mathbf{K}_n^{t\phi} + \tilde{\mathbf{R}}_n^{\phi\theta}\mathbf{K}_n^{\phi\phi}\right)\sin(n\phi^{far}) \tag{77c}$$

and

$$E^{sc,\phi\phi}(\mathbf{r}) \overset{r\to\infty}{\sim} -\frac{jkZ_0e^{-jkr}}{4\pi kr}\left[\tilde{\mathbf{R}}_0^{\phi\phi}\mathbf{K}_0^{\phi\phi} + 2\sum_{n=1}^{N}\left(\tilde{\mathbf{R}}_n^{t\phi}\mathbf{K}_n^{t\phi} + \tilde{\mathbf{R}}_n^{\phi\phi}\mathbf{K}_n^{\phi\phi}\right)\cos(n\phi^{far})\right]. \tag{77d}$$

The radar cross section σ is defined as

$$\sigma^{pq} = \lim_{r\to\infty} 4\pi r^2 \frac{|\, E^{sc,pq}\,|^2}{|\, \mathbf{E}^{inc,q}\,|^2} \tag{78}$$

where $p : \theta$ or ϕ, denotes the component of the far scattered field, and $q : \theta$ (TM) or ϕ (TE), indicates the polarization of the incident electric field.

2.8 Choice of the Number of Fourier Modes for Expansion and Testing Functions.

The ϕ dependence of the current given by (19) is expressed as a summation from $-N$ to N of the Fourier modes $e^{jn\phi}$. The value of N can be set equal to the number of Fourier modes sufficient to represent, to the desired accuracy, the ϕ variation of the tangential component of the incident electric field on the surface of the BOR. Let a be the largest value of ρ of a point (ρ, z) on the generating curve of the BOR. Then from (15), (16), and (17) it can be seen that the ϕ variation of the incident field along the circle on the BOR corresponding to the point (a, z) is given by

$$f(\phi) = \cos\phi e^{jka\sin\theta^{inc}\cos\phi} \quad \text{or} \quad f(\phi) = \sin\phi e^{jka\sin\theta^{inc}\cos\phi}. \tag{79}$$

For axial incidence $\theta^{inc} = 0$ and $f(\phi)$ equals $\cos\phi$ or $\sin\phi$ so that only the $e^{\pm j\phi}$ modes are needed. For oblique incidence, we can express $f(\phi)$ as the Fourier series

$$f(\phi) = \sum_{-N}^{N} c_n e^{jn\phi} \tag{80a}$$

with

$$c_n = \frac{1}{2\pi} \int_0^{2\pi} f(\phi) e^{-jn\phi} d\phi \tag{80b}$$

from which, with (79) and (58),

$$| c_n | = \frac{1}{2} | J_{n+1}(ka \sin\theta^{inc}) \pm J_{n-1}(ka \sin\theta^{inc}) | . \tag{81}$$

As n increases beyond $ka \sin\theta^{inc}$, $| J_n(ka \sin\theta^{inc}) |$ decreases rapidly and it suffices to choose

$$N = I + M \tag{82}$$

where

$$I = \text{Int}[(1+\alpha) ka \sin\theta^{inc}], \quad 0 < \alpha \ll 1 \tag{83}$$

and M is the smallest integer for which

$$\frac{J_N(ka \sin\theta^{inc})}{J_I(ka \sin\theta^{inc})} \leq \epsilon \tag{84}$$

with ϵ a small positive number depending on the desired accuracy. If the value of N given by (82) is plotted as a function of $\text{Int}[ka \sin\theta^{inc}]$ the plot is found to be almost linear. For $\epsilon = 0.005$, for example,

$$N \approx \text{Int}[1.04 ka \sin\theta^{inc}] + 7. \tag{85}$$

A similar expression

$$N \approx \text{Int}[k^+(a \sin\theta) + \lambda] \tag{86}$$

with k^+ denoting a value a few percent larger than k was obtained by Yaghjian [11] for the reciprocal problem of estimating the number of angular modes needed to represent the far field of a radiator in the θ direction.

2.9 Approximation of Derivatives

To approximate the derivatives in (36), (43), and (48) we employ a quadratic Lagrangian interpolation polynomial [12]. Recall that in (24) $K_n^t(t)$ and $K_n^\phi(t)$ were approximated using pulse basis functions. The values of $\rho K_n^t(t)$ and $(1/\rho)K_n^\phi(t)$ at the discrete values $t = t_j, j = 1, \cdots, M$ must then serve as the basis for approximating the derivatives. To do this we fit quadratic polynomials $q^t(t)$ and $q^\phi(t)$ through three consecutive values of ρK_n^t and $(1/\rho)K_n^\phi$ respectively:

$$q^t(t) = \rho_{j-1} K_n^t(t_{j-1}) \frac{(t-t_j)(t-t_{j+1})}{(t_{j-1}-t_j)(t_{j-1}-t_{j+1})} + \rho_j K_n^t(t_j) \frac{(t-t_{j-1})(t-t_{j+1})}{(t_j-t_{j-1})(t_j-t_{j+1})}$$

$$+\rho_{j+1}K_n^t(t_{j+1})\frac{(t-t_{j-1})(t-t_j)}{(t_{j+1}-t_{j-1})(t_{j+1}-t_j)} \tag{87a}$$

and

$$q^\phi(t)=\frac{1}{\rho_{j-1}}K_n^\phi(t_{j-1})\frac{(t-t_j)(t-t_{j+1})}{(t_{j-1}-t_j)(t_{j-1}-t_{j+1})}+\frac{1}{\rho_j}K_n^\phi(t_j)\frac{(t-t_{j-1})(t-t_{j+1})}{(t_j-t_{j-1})(t_j-t_{j+1})}$$

$$+\frac{1}{\rho_{j+1}}K_n^\phi(t_{j+1})\frac{(t-t_{j-1})(t-t_j)}{(t_{j+1}-t_{j-1})(t_{j+1}-t_j)}. \tag{87b}$$

Then

$$\frac{d}{dt}\left[\rho K_n^t(t)\right]_{t=t_j}\approx\frac{d}{dt}q^t(t_j)=\rho_{j-1}K_n^t(t_{j-1})\frac{2t_j-(t_j+t_{j+1})}{(t_{j-1}-t_j)(t_{j-1}-t_{j+1})}$$

$$+\rho_jK_n^t(t_j)\frac{2t_j-(t_{j-1}+t_{j+1}}{(t_j-t_{j-1})(t_j-t_{j+1})}+\rho_{j+1}K_n^t(t_{j+1})\frac{2t_{j+1}-(t_{j-1}+t_j)}{(t_{j+1}-t_{j-1})(t_{j+1}-t_j)} \tag{88a}$$

$$\frac{d}{dt}\left[\frac{1}{\rho}K_n^\phi(t)\right]_{t=t_j}\approx\frac{d}{dt}q^\phi(t_j)=\frac{1}{\rho_{j-1}}K_n^\phi(t_{j-1})\frac{2t_j-(t_j+t_{j+1})}{(t_{j-1}-t_j)(t_{j-1}-t_{j+1})}$$

$$+\frac{1}{\rho_j}K_n^\phi(t_j)\frac{2t_j-(t_{j-1}+t_{j+1}}{(t_j-t_{j-1})(t_j-t_{j+1})}+\frac{1}{\rho_{j+1}}K_n^\phi(t_{j+1})\frac{2t_{j+1}-(t_{j-1}+t_j)}{(t_{j+1}-t_{j-1})(t_{j+1}-t_j)} \tag{88b}$$

and

$$\frac{d^2}{dt^2}\left[\rho K_n^t)\right]_{t=t_j}\approx\frac{d^2}{dt^2}q^t(t_j)=\frac{2\rho_{j-1}K_n^t(t_{j-1})}{(t_{j-1}-t_j)(t_{j-1}-t_{j+1})}+\frac{2\rho_jK_n^t(t_j)}{(t_{j+1}-t_{j-1})(t_{j+1}-t_j)}$$

$$+\frac{2\rho_{j+1}K_n^t(t_{j+1})}{(t_{j+1}-t_{j-1})(t_{j+1}-t_j)}. \tag{88c}$$

These approximations are of the form (37) and (38).

3 NUMERICAL RESULTS

The analysis presented in Section 2 was implemented in a FORTRAN computer program which was then used to obtain numerical results for several different BOR's. In this section we show some representative results using the LEFIE to calculate scattering from a prolate spheroid. The geometry of the spheroid is shown in Figure 4. The semi-major axis of the spheroid is a and the semi-minor axis is b. For the calculations we show, $ka = 20$ and $kb = 10$. The TM illuminating plane wave makes an angle of 45° with the major axis of the spheroid. For these values of ka and kb no spurious resonances are encountered. (See end of Section 2.2.)

The solid curve in Figure 5 shows the E-plane pattern calculated with the combined field integral equation (CFIE) implemented in the computer code CICERO [13] using a discretization of the spheroid generating curve of 40 points/λ. The dotted curve in Figure 5 is the pattern obtained by solving the conventional EFIE with the Galerkin form of the method of moments and overlapping triangle basis functions with a point density of 20 points/λ. The dot-dashed curve and the dashed curve in Figure 5 are the patterns obtained solving

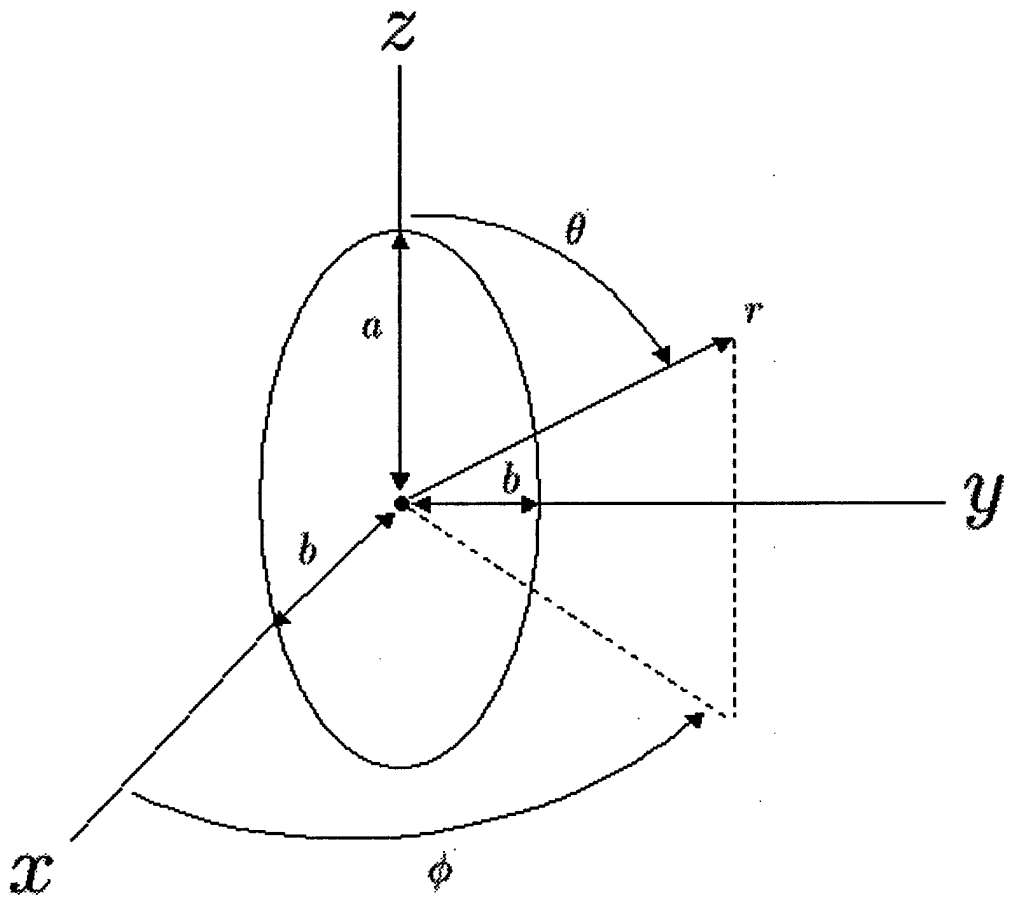

Figure 4: Geometry of the prolate spheroid.

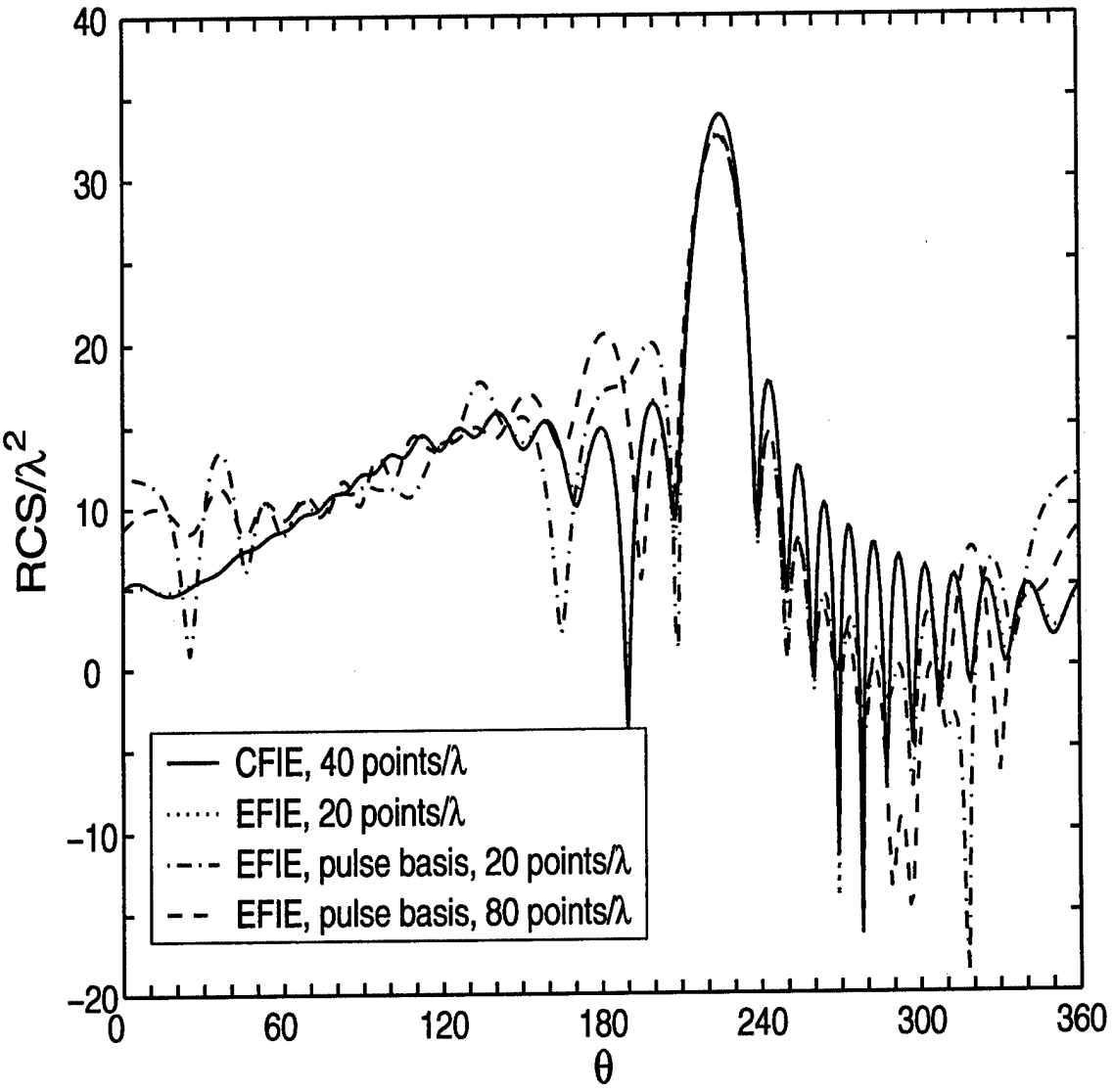

Figure 5: E-plane pattern of a prolate spheroid with $ka = 20$ and $kb = 10$ illuminated by a TM plane wave incident at an angle of 45° with the major axis, as calculated by the CFIE at a density of 40 points/λ, by the EFIE solved with overlapping triangle basis functions at a density of 20 points/λ, and by the EFIE solved with pulse basis functions and point matching with a density of 20 points/λ and 80 points/λ.

the conventional EFIE with pulse basis functions and point matching at point densities of 20 points/λ and 80 points/λ, respectively. We note that the CFIE and EFIE solved with overlapping triangle basis functions yield results that agree closely, but the patterns obtained with pulse basis functions and point matching are highly inaccurate. Moreover, these pulse basis function patterns are not significantly improved upon by considerably increasing the point density.

In contrast with the very poor results obtained when the conventional EFIE is solved using pulse basis functions and point matching, in Figure 6 we show the spheroid patterns obtained solving the conventional EFIE with the method of moments and overlapping triangle basis functions with a density of 20 points/λ, and the patterns obtained by solving the LEFIE with pulse basis functions and point matching at densities of 40 pointsλ and 20 points/λ. The LEFIE solved at a density of 40 points/λ yields a pattern quite close to the conventional EFIE pattern obtained at a density of 20 points/λ. The LEFIE solved with a density of 20 points/λ, however, has some pattern errors of approximately 1.5 dB. The point density required to obtain results with the LEFIE comparable in accuracy to those obtained with the conventional EFIE can be improved upon considerably by the stratagem of using a higher point density for only a very small region – say $\lambda/4$ – in the vicinity of the ends of the spheroid generating curve, and a low point density elsewhere as shown in Figure 7. In the LEFIE pattern shown in Figure 7 a density of 80 points/λ was used close to the ends of the spheroid generating curve (i.e., the poles of the spheroid) and a density of 20 points/λ was used elsewhere. The reason why a high point density may be required at the ends of the BOR generating curve is that the finite difference approximation of the derivatives used in solving the LEFIE is less accurate at the beginning and end of the generating curve because one-sided derivative approximations must be used there. Using a higher point density at the ends of the generating curve compensates for the use of one-sided finite difference derivative approximations.

4 SUMMARY

Unlike the magnetic-field integral equation, the conventional form of the electric-field integral equation cannot be solved accurately using pulse-basis functions and point matching. It can be demonstrated that it is the highly singular kernel of the EFIE, rather than the derivatives of the current, that precludes the use of the pulse-basis-function, point-matching MOM. A new form of the EFIE has been derived whose kernel has no greater singularity than the free-space Green's function. This new low-order singularity form of the EFIE, the LEFIE, has been solved for a perfectly electrically conducting body of revolution using the pulse-basis function point-matching MOM, and a computer program has been written to implement the solution. Derivatives of the current are approximated with finite differences using a quadratic Lagrangian interpolation polynomial. This simple solution of the LEFIE is contingent, however, on the vanishing of a linear integration term that appears when the original EFIE is transformed to obtain the LEFIE. The vanishing of this linear integration term restricts the applicability of the LEFIE to smooth closed scatterers without tips, edges, or any other features that might result in a discontinuous or unbounded surface charge density, its surface derivative, and the sum of the reciprocals of the principal radii of

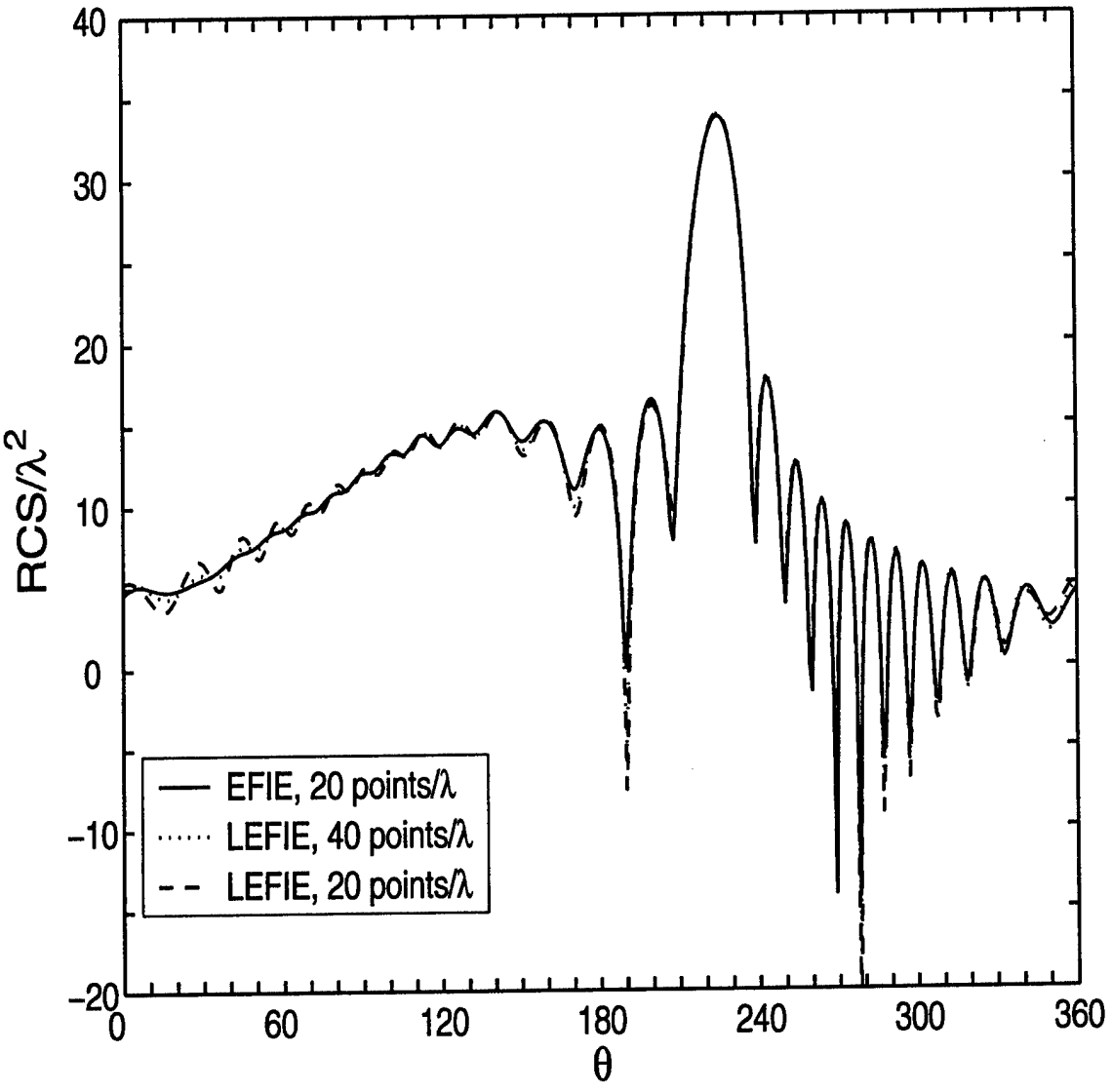

Figure 6: E-plane pattern of a prolate spheroid with $ka = 20$ and $kb = 10$ illuminated by a TM plane wave incident at an angle of 45° with the major axis, as calculated by the EFIE solved with overlapping triangle basis functions at a density of 20 points/λ, and by the LEFIE solved with pulse basis functions and point matching at a density of 40 points/λ and 20 points/λ.

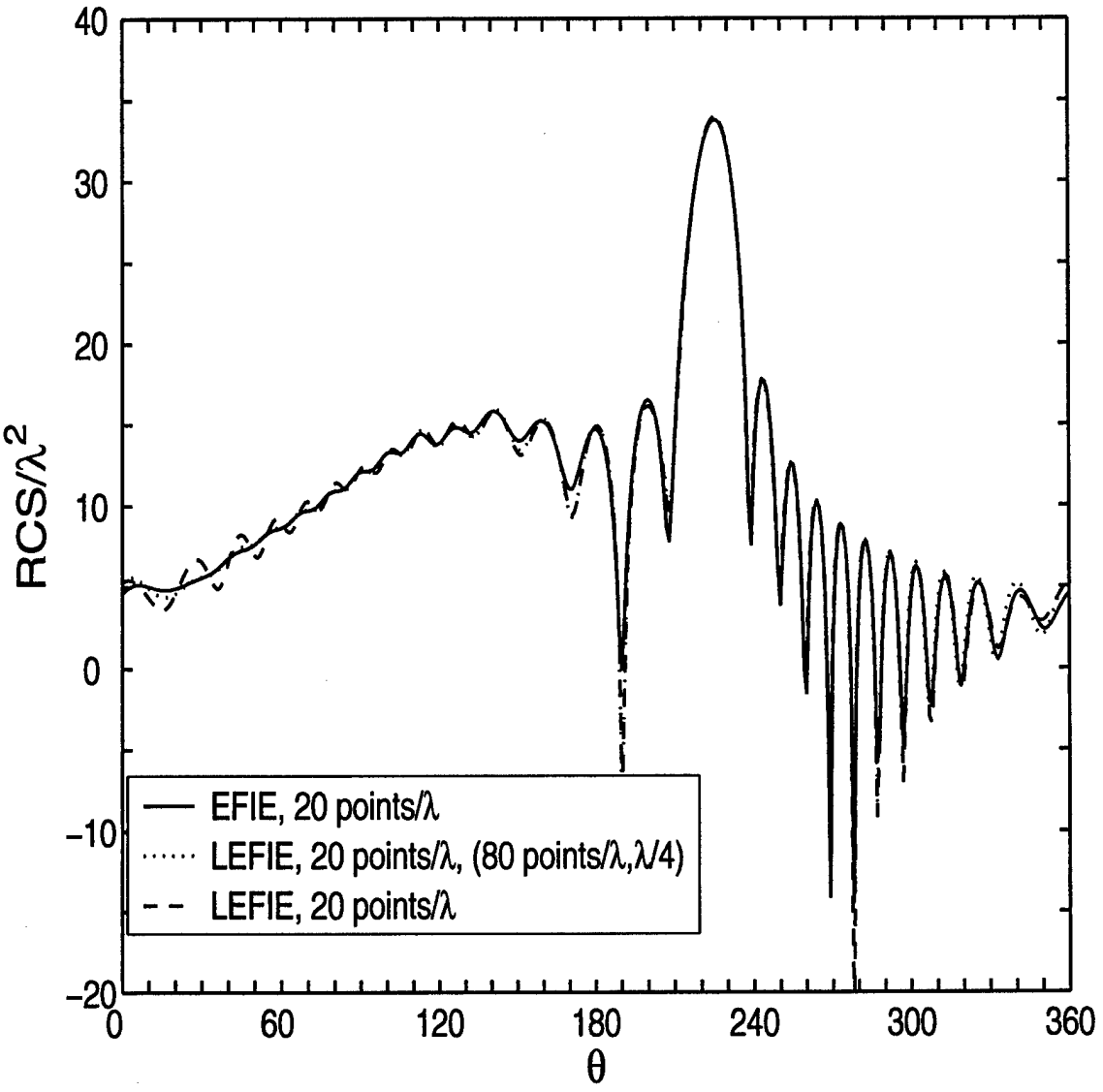

Figure 7: E-plane pattern of a prolate spheroid with $ka = 20$ and $kb = 10$ illuminated by a TM plane wave incident at an angle of 45° with the major axis, as calculated by the EFIE solved with overlapping triangle basis functions at a density of 20 points/λ, by the LEFIE solved with pulse basis functions and point matching at a density of 80 points/λ in an interval of $\lambda/4$ at either end of the spheroid generating curve and 20 points/λ elsewhere, and by the LEFIE at a uniform density of 20 points/λ.

curvature, or a discontinuous unit normal vector to the surface. Bistatic RCS calculations performed for a prolate spheroid demonstrate that results comparable in accuracy to the conventional EFIE can be obtained with the LEFIE using pulse-basis functions and point matching provided that a higher density of points is used close to the ends of the BOR generating curve to compensate for the use of one-sided finite difference approximations of the first and second derivatives of the current.

References

[1] A.W. Maue, "On the formulation of a general scattering problem by means of an integral equation," *Z. Phys.*, vol. 126, pp. 601–618, 1949.

[2] J. Van Bladel, *Electromagnetic Fields*, McGraw-Hill, New York, 1964.

[3] A.D. Yaghjian, "Augmented electric- and magnetic-field integral equations," *Radio Science*, vol. 16, 987–1001, November-December 1981.

[4] J.R. Mautz and R.F. Harrington, "H-field, E-field, and combined-field solutions for conducting bodies of revolution'" *Arch. Math. Ubertragungtech.*, vol. 32, pp. 157–164, 1978.

[5] A.D. Yaghjian and M.B. Woodworth, "Derivation, application and conjugate gradient solution of the dual-surface integral equations for three-dimensional, multiwavelength perfect conductors," in *PIER 5, Progress in Electromagnetics Research: Applications of the Conjugate Gradient Method to Electromagnetics and Signal Analysis*, T. Sarkar, ed., New York: Elsevier, 1991, 103–130.

[6] M.B. Woodworth and A.D. Yaghjian, "Multiwavelength three-dimensional scattering with dual-surface integral equations," *J. Opt. Soc. Am. A*, vol. 11, pp. 1399–1413, April 1994.

[7] A.F Peterson, S.L. Ray, and R. Mittra, *Computational Methods for Electromagnetics*, New York: IEEE Press, 1998.

[8] R.A. Shore and A.D. Yaghjian, *"Dual Surface Electric Field Equation"*, Air Force Research Laboratory Report No. AFRL-SN-HS-TR-2001-013, 2001.

[9] R.A. Shore and A.D. Yaghjian,"Dual-Surface Integral Equations in Electromagnetic Scattering," Proceedings International Union of Radio Science (URSI) 27th General Assembly, Maastricht, The Netherlands, August 2002.

[10] C.A. Balanis, *Advanced Engineering Electromagnetics*, New York: John Wiley, 1989.

[11] A.D. Yaghjian, *Near Field Antenna Measurements on a Cylindrical Surface: A Source Scattering Matrix Formulation*, NBS Technical Note 696, 1977.

[12] C.E. Pearson, *Numerical Methods in Engineering and Science*, New York: Van Nostrand Reinhold, 1986.

[13] J.M. Putnam and L.N. Medgyesi-Mitschang, *Combined Field Integral Equation Formulation for Axially Inhomogeneous Bodies of Revolution*, McDonnell Douglas Research Laboratories MDC Report No. QA003, December 1987.